Aluminum Properties and Physical Metallurgy
John E. Hatch editor, p 134-199
DOI: 10.1361/appm1984p134

CHAPTER 5

METALLURGY OF HEAT TREATMENT AND GENERAL PRINCIPLES OF PRECIPITATION HARDENING*

The heat treatable alloys contain amounts of soluble alloying elements that exceed the equilibrium solid solubility limit at room and moderately higher temperatures. The amount present may be less or more than the maximum that is soluble at the eutectic temperature. Figure 1, which shows a portion of the aluminum-copper equilibrium diagram, illustrates these two conditions and the fundamental solution-precipitation relationships involved. Two alloys containing 4.5 and 6.3% copper are represented by the vertical dashed lines (a) and (b). The solubility relationships and heat treating behavior of these compositions approximate those of commercial alloys 2025 and 2219, and the principles apply to the other heat treatable alloys.

The diagram in Fig. 1 shows that, regardless of the initial structure, holding the 4.5% copper alloy at 515 to 550 °C (960 to 1020 °F) until equilibrium is attained causes the copper to go completely into solid solution. This operation is generally known as "solution heat treating." If the temperature is then reduced to below 515 °C (960 °F), the solid solution becomes supersaturated, and there is a tendency for the excess solute over the amount actually soluble at the lower temperature to precipitate. The driving force for precipitation increases with the degree of supersaturation and, consequently, with decreasing temperature; the rate also depends on atom mobility, which is reduced as temperature decreases. Although the solution-precipitation reaction is fundamentally reversible with temperature change, in many alloys transition structures form during precipitation but not during solution. Mechanical and physical properties depend not only on whether the solute is in or out of solution but also on specific atomic arrangements, as well as on size and dispersion of any precipitated phases.

Referring again to Fig. 1, the alloy with 6.3% copper, which exceeds the maximum content soluble at the eutectic temperature, consists of a solid solution plus additional undissolved $CuAl_2$ when heated to slightly below the eutectic temperature. The solid solution has a higher copper concentration than that of the 4.5% copper alloy if the temperature exceeds 515 °C (960 °F). The increased copper in solid solution provides greater driving force for precipitation at lower temperatures and increases

*This chapter was revised by a team comprised of J.T. Staley, Alcoa Technical Center; R.F. Ashton, Reynolds Metals Co.; I. Broverman, Kaiser Aluminum & Chemical Corp.; and P.R. Sperry, Consolidated Aluminum Corp. The original chapter was authored by H.Y. Hunsicker, Alcoa Research Laboratories.

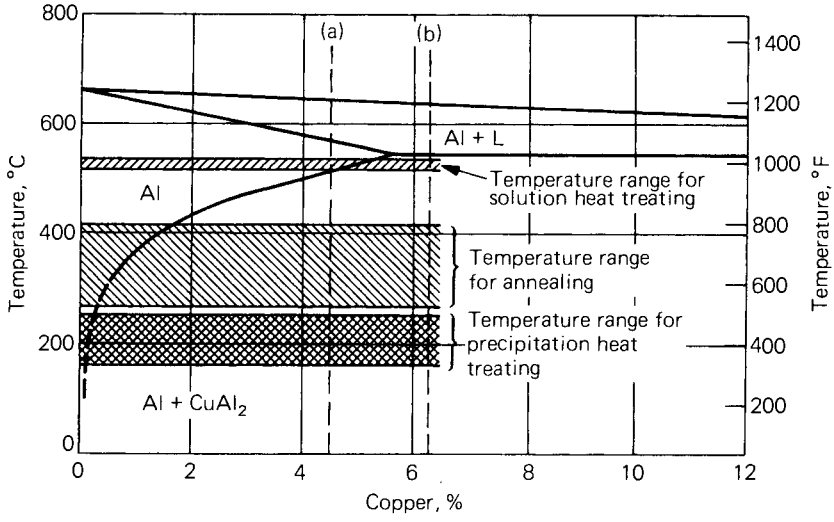

Fig. 1. Partial equilibrium diagram for aluminum-copper alloys, with temperature ranges for heat treating operations.

the magnitude of property changes that may occur. The $CuAl_2$ that is not dissolved at the high temperature, while remaining essentially unaltered through heating and cooling, perceptibly raises the overall strength level.

Although the simple aluminum-copper binary phase diagram is convenient for illustrating principles, the presence of an impurity or other alloying element alters the real values of solid solubility limits and the equilibrium or nonequilibrium solidus temperatures. Familiarity with ternary and more complex phase diagrams is essential for a deeper understanding of heat treatment phenomena. The additional degrees of freedom resulting from each component added to a binary system produce phase compositions and transition temperatures that cannot be depicted readily by the two-dimensional binary diagram.

The solid solution formed at a high temperature may be retained in a supersaturated state by cooling with sufficient rapidity to minimize precipitation of the solute atoms as coarse, incoherent particles. Controlled precipitation of fine particles at room or elevated temperatures after the quenching operation is used to develop the mechanical properties of the heat treated alloys.

Most alloys exhibit property changes at room temperature after quenching. This is called "natural aging" and may start immediately after quenching, or after an incubation period. The rates vary from one alloy to another over a wide range, so that the approach to a stable condition may require only a few days or several years. Precipitation can be accelerated in these alloys, and their strengths further increased, by heating above room temperature; this operation is referred to as "artificial aging" or "precipitation heat treating."

Alloys with slow precipitation reactions at room temperature must be precipitation heat treated to attain the high strengths of which they are capable. In certain alloys, considerable additional increase in strength can

be obtained by imposing controlled amounts of cold work on the product after quenching. A portion of the increase in strength obtained by this practice is attributed to strain hardening, but when cold working is followed by precipitation heat treating, the precipitation effects are greatly accentuated. As is apparent from the descriptions of the Aluminum Association temper designations applicable to heat treatable alloys below, other combinations and sequences of cold working and precipitation heat treatments are used; these are discussed subsequently in more detail. The basic temper designations are as follows:

F **As fabricated:** Applies to the products of shaping processes in which no special control over thermal conditions or strain-hardening is used. For wrought products, there are no mechanical property limits

O **Annealed:** Applies to wrought products that are annealed to obtain the lowest strength temper and to cast products that are annealed to improve ductility and dimensional stability. The O may be followed by a digit other than zero

W **Solution heat treated:** An unstable temper applicable only to alloys which spontaneously age at room temperature after solution heat treatment. This designation is specific only when the period of natural aging is indicated; for example: W $^1/_2$h

T **Thermally treated to produce stable tempers other than F, O, or H:** Applies to products which are thermally treated, with or without supplementary strain hardening, to produce stable tempers

The T is always followed by one or more digits. A period of natural aging at room temperature may occur between or after the operations listed for the T tempers. Control of this period is exercised when it is metallurgically important. Numerals 1 through 10 indicate specific sequences of treatments:

T1 **Cooled from an elevated-temperature shaping process and naturally aged to a substantially stable condition:** Applies to products that are not cold worked after cooling from an elevated-temperature shaping process, or in which the effect of cold work in flattening or straightening may not be recognized in mechanical property limits

T2 **Cooled from an elevated-temperature shaping process, cold worked, and naturally aged to a substantially stable condition:** Applies to products that are cold worked to improve strength after cooling from an elevated-temperature shaping process, or in which the effect of cold work in flattening or straightening is recognized in mechanical property limits

T3 **Solution heat treated, cold worked, and naturally aged to a substantially stable condition:** Applies to products that are cold worked to improve strength after solution heat treatment, or in which the effect of cold work in flattening or straightening is recognized in mechanical property limits

T4 **Solution heat treated and naturally aged to a substantially stable condition:** Applies to products that are not cold worked after solution heat treatment, or in which the effect of cold work in flattening or straightening may not be recognized in mechanical property limits

T5 **Cooled from an elevated-temperature shaping process and then artificially aged:** Applies to products that are not cold worked after cooling from an elevated-temperature shaping process, or in which the effect of cold work in flattening or straightening may not be recognized in mechanical property limits

T6 **Solution heat treated and then artificially aged:** Applies to products that are not cold worked after solution heat treatment, or in which the effect of cold work in flattening or straightening may not be recognized in mechanical property limits

T7 **Solution heat treated and stabilized:** Applies to products that are stabilized after solution heat treatment to carry them beyond the point of maximum strength to provide control of some special characteristic

T8 **Solution heat treated, cold worked, and then artificially aged:** Applies to products that are cold worked to improve strength, or in which the effect of cold work in flattening or straightening is recognized in mechanical property limits

T9 **Solution heat treated, artificially aged, and then cold worked:** Applies to products that are cold worked to improve strength

T10 **Cooled from an elevated-temperature shaping process, cold worked, and then artificially aged:** Applies to products that are cold worked to improve strength, or in which the effect of cold work in flattening or straightening is recognized in mechanical property limits

Solution heat treatment is achieved by heating cast or wrought products to a suitable temperature, holding at that temperature long enough to allow constituents to enter into solid solution, and cooling rapidly enough to hold the constituents in solution. Some 6000 series alloys attain the same specified mechanical properties whether furnace solution heat treated or cooled from an elevated-temperature shaping process at a rate rapid enough to hold constituents in solution. In such cases the temper designations T3, T4, T6, T7, T8, and T9 are used to apply to either process and are appropriate designations.

The following designations involving additional digits are assigned to stress-relieved tempers of wrought products:

T—51 **Stress relieved by stretching:** Applies to the following products when stretched the indicated amounts after solution heat treatment or cooling from an elevated-temperature shaping process:

Plate ..... $1\frac{1}{2}$ to 3% permanent set
Rod, bar, shapes,
extruded tube ..... 1 to 3% permanent set
Drawn tube ..... $\frac{1}{2}$ to 3%

Applies directly to plate and rolled or cold finished rod and bar. These products receive no further straightening after stretching

Applies to extruded rod, bar, shapes, and tube and to drawn tube when designated as follows:

T—510: Products that receive no further straightening after stretching

T—511: Products that may receive minor straightening after stretching to comply with standard tolerances

T—52 **Stress-relieved by compressing:** Applies to products that are stress-relieved by compressing after solution heat treatment or cooling from an elevated-temperature shaping process to produce a permanent set of 1 to 5%

T—54 **Stress-relieved by combined stretching and compressing:** Applies to die forgings that are stress relieved by restriking cold in the finish die

The same digits (51, 52, 54) may be added to the designation W to indicate unstable solution heat treated and stress-relieved tempers. The following temper designations have been assigned for wrought products heat treated from O or F temper to demonstrate response to heat treatment:

T42 Solution heat treated from the O or F temper to demonstrate response to heat treatment, and naturally aged to a substantially stable condition

T62 Solution heat treated from the O or F temper to demonstrate response to heat treatment, and artificially aged

Temper designations T42 and T62 may also be applied to wrought products heat treated from any temper by the user when such heat treatment results in the mechanical properties applicable to these tempers.

The increases in strength of the alloys that exhibit natural aging either continue indefinitely at room temperature or stabilize. Aging at elevated temperatures is characterized by a different behavior in which strength and hardness increase to a maximum and subsequently decrease. The softening effects, observed as more complete precipitation, occur during extended aging at elevated temperatures and are referred to as "overaging." They are as significant as the strengthening effects associated with the preceding stages of precipitation. Softening results from changes in both the type and size of precipitated particles and from dilution of the solid solution. The softest, lowest strength condition of the heat treatable alloys is obtained by annealing treatments that precipitate the maximum amount of solute as relatively large, widely spaced, incoherent particles.

Alloy hardening and softening attributable to precipitation are illustrated by the isothermal aging curves in Fig. 2. These curves show typical effects of time and temperature that are basic to the heat treating process and influence the selection of conditions to achieve various mechanical properties. Some of the important features illustrated are:

- Hardening can be greatly retarded or suppressed indefinitely by lowering the temperature
- The rates of hardening and subsequent softening increase with increasing temperature
- Over the temperature range in which a maximum strength can be observed, the level of the maximum generally decreases with increasing temperature

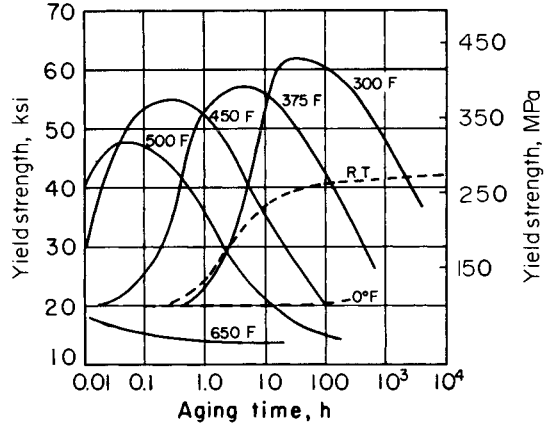

Fig. 2. Representative isothermal aging curves for alloy 2014-T4.

- At sufficiently high temperatures no hardening is observed, and precipitation causes an initial and continued softening

In selecting combinations of time and temperature for commercial processing to achieve maximum strength and hardness, the features given above are considered, together with certain limitations imposed by economic factors. Adequate control favors avoiding short-time, high-temperature combinations, which are on steeply sloping portions of the aging curves, and leads to a preference for temperatures that provide a broad maximum. The variations in aging behavior shown in Fig. 2 can now be related to Fig. 1, which indicates the temperature ranges for the different basic heat treating operations. Thus, the temperature range for annealing produces effects of the type illustrated by the 345 °C (650 °F) curve in Fig. 2, whereas the range for precipitation heat treating is associated with aging characteristics of the type shown by the curves for 150 to 260 °C (300 to 500 °F).

NATURE OF PRECIPITATES AND SOURCES OF HARDENING

Intensive research over many decades has resulted in a progressive accumulation of knowledge concerning the atomic and crystallographic structural changes that occur in supersaturated solid solutions during precipitation and the mechanisms through which the structures form and alter alloy properties. In most precipitation-hardenable systems, a complex sequence of time- and temperature-dependent changes is involved. At relatively low temperatures and during initial periods of artificial aging at moderately elevated temperatures, the principal change is a redistribution of solute atoms within the solid-solution lattice to form clusters or GP (Guinier-Preston) zones that are considerably enriched in solute. This local segregation of solute atoms produces a distortion of the lattice planes, both within the zones and extending for several atom layers into the matrix. With an increase in the number or density of zones, the degree of disturbance of the regularity and periodicity of the lattice increases. The strengthening effect of the zones results from the additional interference with the motion of dislocations when they cut the GP zones. This may be because of chemical strengthening (the production of a new particle-matrix interface) and the increase in stress required to move a dislocation through a region distorted by coherency stresses. The progressive strength increase with natural aging time has been attributed to an increase in the size of the GP zones in some systems and to an increase in their number in others.

In most systems, as aging temperatures or time are increased, the zones are either converted into or replaced by particles having a crystal structure distinct from that of the solid solution and also different from the structure of the equilibrium phase. These are referred to as transition precipitates. In most alloys, they have specific crystallographic orientation relationships with the solid solution, such that the two phases remain coherent on certain planes by adaptation of the matrix through local elastic strain. The strengthening effects of these semicoherent transition structures are related to the impedance to dislocation motion provided by the presence of lattice strains and precipitate particles. Strength continues to increase

as the size of these precipitates increases, as long as the dislocations continue to cut the precipitates.

Further progress of the precipitation reaction produces growth of transition phase particles, with an accompanying increase in coherency strains, until the strength of the interfacial bond is exceeded and coherency disappears. This frequently coincides with a change in the structure of the precipitate from transition to equilibrium form. With the loss of coherency strain, strengthening effects are caused by the stress required to cause dislocations to loop around rather than cut the precipitates. Strength progressively decreases with growth of equilibrium phase particles and an increase in interparticle spacing.

Kinetics of Solution and Precipitation. The relative rates at which solution and precipitation reactions occur with different solutes depend on the respective diffusion rates, in addition to solubilities and alloying contents. Bulk diffusion coefficients for several of the commercially important alloying elements in aluminum were determined by various experimental methods, including activation and electron microprobe analyses. A summary of these data, including those for self-diffusion, is shown in Fig. 3. Copper, magnesium, silicon, and zinc, which are the principal solutes involved in precipitation-hardening reactions, have relatively high rates of diffusion in aluminum.

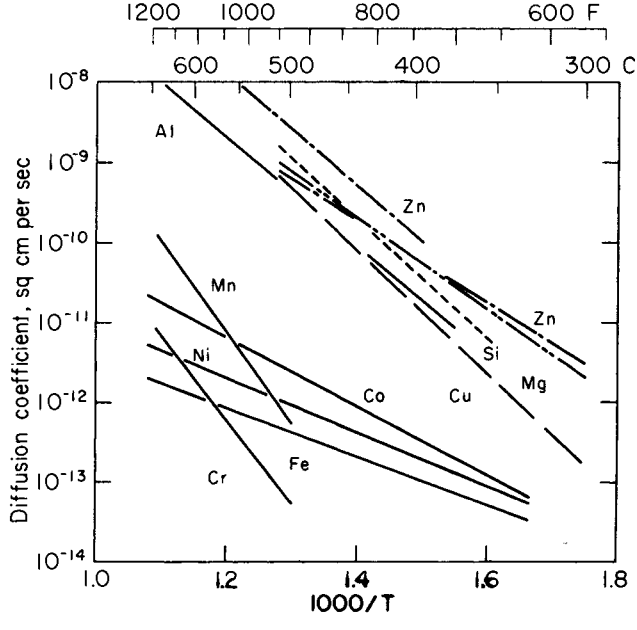

Fig. 3. Diffusion coefficients for various elements in aluminum. Letters in parentheses refer to sources of data. (a) K. Hirano, R.P. Agarwala, and M. Cohen, Acta Metallurgica, *Vol 10, 1962, p 857-863. (b) W.G. Fricke, Jr., Alcoa Research Laboratories. (c) T.S. Lundy and J.F. Murdock,* Journal of Applied Physics, *Vol 33, 1962, p 1671-1673. (d) J.E. Hilliard, B.L. Averbach, and M. Cohen,* Acta Metallurgica, *Vol 1, 1959, p 86-92*

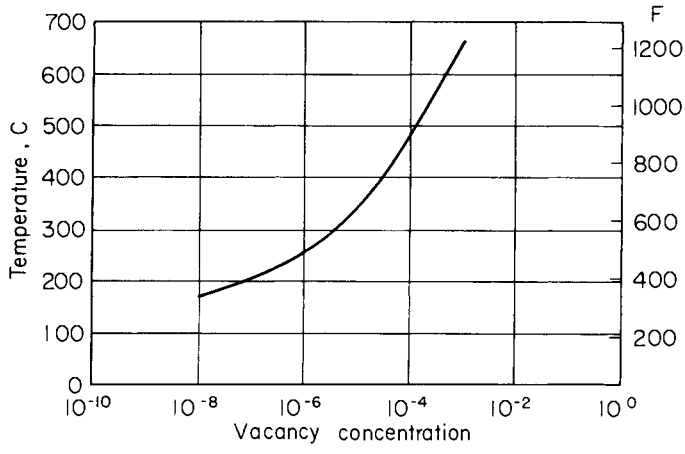

Fig. 4. Equilibrium concentration of vacancies in pure aluminum as a function of temperature. (D. Altenpohl, Aluminium, *Vol 37, 1961, p 401-411)*

Vacancies. Considerable experimental evidence accumulated during the past 20 years strongly indicates that significant numbers of the lattice positions in most crystalline solids are not occupied by atoms. These vacant lattice sites are called "vacancies" (Ref 1). Diffusion of the substitutional solid-solution-forming elements, as well as self-diffusion, is believed to occur primarily by a vacancy exchange mechanism. Vacancies have a particularly significant role in the formation of GP zones. In order to explain the rates of zone formation that are observed at relatively low temperatures, diffusion rates several orders of magnitude greater than those obtained by extrapolating rates measured at higher temperatures are required (Ref 2). Precise measurements of electrical resistivities and relative changes in density and lattice conditions with temperature have been used to ascertain an equilibrium concentration of vacancies in aluminum that varies with temperature, approximately as illustrated in Fig. 4.

The increased low-temperature solute mobility required to account for the high rates of zone formation was explained by a vacancy-assisted diffusion mechanism, made possible by the retention of a nonequilibrium high vacancy concentration at the low temperature (Ref 3). In addition to this fundamental role of vacancies, several specific interactions between vacancies and various solute atoms influence aging kinetics and make the effects of trace elements important. Magnesium appears to play a special role in this process. Because of its large atomic diameter, magnesium-vacancy complexes are readily formed and make retention of excess vacancies during quenching easier. The availability of these vacancies has a marked effect on precipitation kinetics and strengthening potential.

Nucleation. The formation of zones can occur in an essentially continuous crystal lattice by a process of homogeneous nucleation. Several investigations provide evidence that critical vacancy concentration is required for this process and that a nucleation model involving vacancy-solute atom clusters is consistent with certain effects of solution temperature and quenching rate (Ref 4-10).

The nucleation of a new phase is greatly influenced by discontinuities in the lattice such as grain boundaries, subgrain boundaries, dislocations, and interphase boundaries. Because these sites are locations of greater disorder and higher energy than the solid-solution matrix, they nucleate either transition or equilibrium precipitates. The solute that precipitates in this uncontrolled manner during the quench is unavailable for subsequent precipitation either at room or elevated temperatures, so precipitation during the quench can affect the development of properties. The effect on strength of precipitating during the quench onto grain boundaries, subgrain boundaries, and scattered particles on the order of 0.5 μm (0.02 mil) or larger is generally negligible. The effects of precipitating onto the fine dispersoid particles (<0.1 μm or <0.004 mil) formed by high temperature precipitation at an earlier stage in the processing, however, can be large when the rate of cooling is not rapid enough. Figure 5 illustrates precipitate formed on one such particle with an accompanying deficiency of precipitate adjacent to the particle. This phenomenon of a

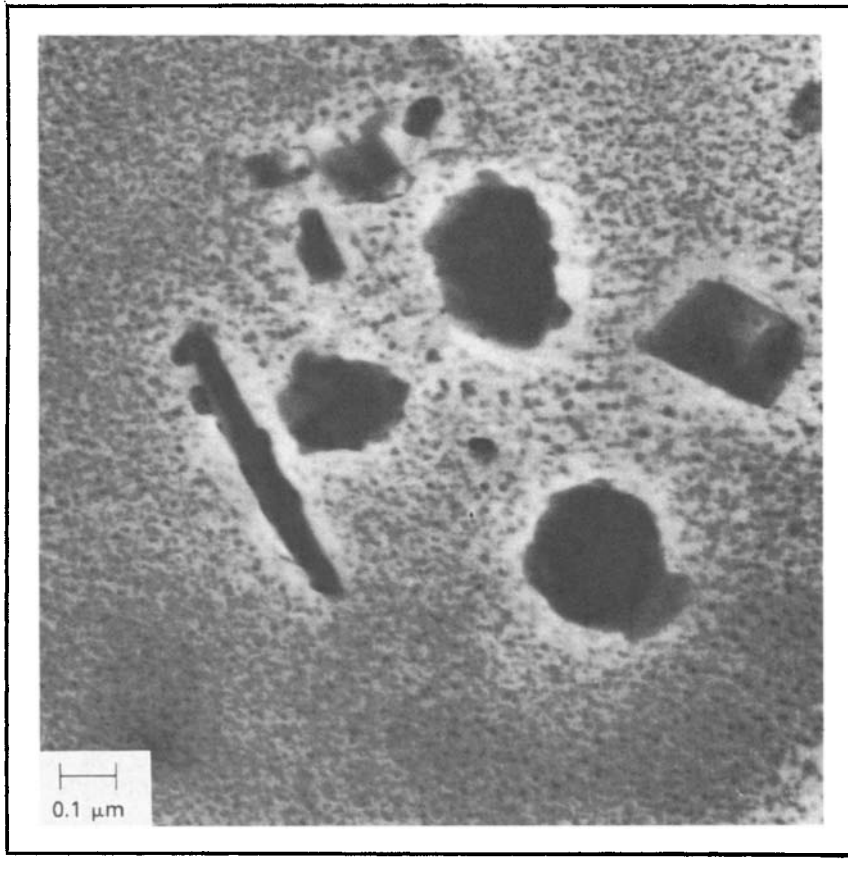

Fig. 5. Transmission electron micrograph of 75-mm (3-in.) thick 7039-T63 plate. Note the precipitate on the dispersoids and the resultant precipitate-free-zone surrounding each dispersoid particle.

precipitate-free zone (PFZ) after slow quenching and aging is attributed to the depletion of solute atoms near the particles and to the scarcity of nucleation sites caused by the migration of vacancies to the particle-matrix boundaries during the quench.

Although precipitates at grain boundaries do not have a large effect on attainable strength, they can have a harmful effect on the corrosion resistance of the material and increase the tendency toward intergranular fracturing. Grain boundary precipitation is frequently accompanied by the development of precipitate-free zones similar to those seen adjacent to dispersoid particles. Electrochemical potential relations between intergranular precipitate particles, precipitate-depleted or GP zone-depleted layers, and grain interiors are fundamental to the electrochemical theory of intergranular stress-corrosion cracking.

Investigations of precipitated structures by transmission electron microscopy have demonstrated that dislocations formed by condensation of vacancies or by introduction of plastic strain are also very active nucleation sites for precipitation (Ref 11). Variations in dislocation density resulting from different quenching rates, as well as the degree of vacancy and solute retention achieved during the quench, are factors in determining the effects of quenching rates on strengthening. The introduction of dislocations by cold working after quenching accelerates precipitation in 2XXX alloys and increases the strength developed during artificial aging. In other alloys, the effects of cold working are either negligible or detrimental, as subsequently discussed in this chapter.

PRECIPITATION IN SPECIFIC ALLOY SYSTEMS

Several commercially important aluminum alloy systems have been subjected to careful investigation of the structures existing at various stages of the precipitation process, and these are briefly described below.

Aluminum-Copper. In these alloys, the hardening observed at room temperature is attributed to localized concentrations of copper atoms forming Guinier-Preston zones, designated GP (1). These consist of two-dimensional copper-rich regions of disk-like shape, oriented parallel to {100} planes. The diameter of the zones is estimated to be 3 to 5 nm (30 to 50 Å) and does not change with aging time at room temperature. The number, however, increases with time, until in the fully aged condition, the average distance between zones is about 100 nm (1000 Å).

At temperatures of 100 °C (212 °F) and higher, the GP (1) zones disappear and are replaced by a structure designated GP (2) or θ″ which, although only a few atom layers in thickness, is considered to be three-dimensional and to have an ordered atomic arrangement. The transition phase, θ′, having the same composition as the stable phase and exhibiting coherency with the solid solution lattice, forms after GP (2), but coexists with it over a range of time and temperature. The final stage in the sequence is the transformation of θ′ into noncoherent equilibrium θ ($CuAl_2$). The structure sequence in aluminum-copper alloys may be diagrammed:

$$SS \rightarrow GP\,(1) \rightarrow GP\,(2) \rightarrow \theta' \rightarrow \theta'' \qquad \text{Eq 1}$$

The correlation of these structures with hardness is illustrated in Fig. 6 for a 4% copper alloy aged at two temperatures. At some temperatures,

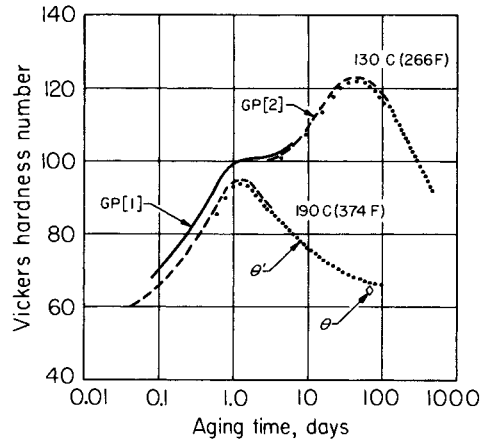

Fig. 6. Correlation of structure and hardness of Al-4% Cu alloy aged at two temperatures. (J.M. Silcock, T.J. Heal, and H.K. Hardy, Journal of the Institute of Metals, *1953-1954, p 82239-82248)*

for example 130 °C (265 °F), the initial hardening from formation of GP (1) is distinguishable from a second stage attributable to GP (2). Maximum hardness and strength occur when the amount of GP (2) is essentially at a maximum, although some contribution may also be provided by θ′. As the amount of θ′ increases, particle growth eventually decreases the coherency strains. This loss in coherency, together with the simultaneous decrease in GP (2), causes overaging. When the noncoherent θ appears, the alloy is softened far beyond the maximum-strength condition.

Aluminum-Copper-Magnesium Alloys. Additions of magnesium to aluminum-copper alloys accelerate and intensify natural age hardening. These were the first heat treatable high-strength aluminum alloys, and they have continued through the years to be among the most popular and useful. Despite their early origin and large-volume production, details of the precipitation mechanisms and structures of aluminum-copper-magnesium alloys are less well developed than for aluminum-copper alloys. Although evidence is strong for the formation of zones during natural aging, it has not been possible to ascertain their form or size. They are believed to consist of groups of magnesium and copper atoms that collect on {110} matrix planes. The apparent acceleration of this process by the addition of magnesium may result from complex interactions between vacancies and the two solutes. Some preparatory pairing of copper and magnesium atoms also has been suggested, and the pairing may contribute to hardening by a mechanism of dislocation pinning.

Aging of 2024-T4 alloy at elevated temperatures produces the transition phase S' (Al_2CuMg), which is coherent on {021} matrix planes, whereas overaging is associated with formation of the equilibrium S phase (Al_2CuMg) and loss of coherency. The precipitation structure sequence may be represented as follows:

$$SS \rightarrow GP \rightarrow S' (Al_2CuMg) \rightarrow S (Al_2CuMg) \qquad \text{Eq 2}$$

Small additions of magnesium significantly strengthen aluminum-copper alloys even though no evidence of S' has been detected after precipitation heat treatments.

Aluminum-Magnesium-Silicon Alloys. Appreciable strengthening in these alloys occurs over an extended period at room temperature. This strengthening probably entails the formation of zones, although they have not been positively detected in the naturally aged state. Short aging times at temperatures up to 200 °C (390 °F) produce x-ray and electron diffraction effects indicating the presence of very fine, needle-shaped zones oriented in the ⟨001⟩ direction of the matrix. Electron microscopy indicated the zones to be approximately 6 nm (60 Å) in diameter and 20 to 100 nm (200 to 1000 Å) in length. Another investigation indicates that the zones are initially of spherical shape and convert to needlelike forms near the maximum strength inflections of the aging curves. Further aging causes apparent three-dimensional growth of the zones to rod-shaped particles with a structure corresponding to a highly ordered Mg_2Si. At higher temperatures, this transition phase, designated β', undergoes diffusionless transformation to the equilibrium Mg_2Si.

No direct evidence of coherency strain is found in either the zone or transition precipitate stages. It has been suggested that the increased resistance to dislocation motion accompanying the presence of these structures arises from the increased energy required to break magnesium-silicon bonds in the zones as dislocations pass through them. Grain boundary precipitate particles of silicon are found at very early stages of aging in alloys having an excess of silicon over the Mg_2Si ratio. The normal precipitation sequence may be diagrammed as follows:

$$SS \rightarrow GP \rightarrow \beta' (Mg_2Si) \rightarrow \beta (Mg_2Si) \qquad \text{Eq 3}$$

Aluminum-Zinc-Magnesium and Aluminum-Zinc-Magnesium-Copper Alloys. The aging of rapidly quenched aluminum-zinc-magnesium alloys from room temperature to relatively low aging temperatures is accompanied by the generation of GP zones having an approximately spherical shape. With increasing aging time, GP zones increase in size, and the strength of the alloy increases. Figure 7 shows GP zones in alloy 7075 that attained a diameter of 1.2 nm (12 Å) after 25 years at room temperature. After that time, the yield strength was about 95% of the value after standard T6 aging. Extended aging at temperatures above room temperature transforms the GP zones in alloys with relatively high zinc-magnesium ratios into the transition precipitate known as η' or M′, the precursor of the equilibrium $MgZn_2$, η, or M phase precipitate. The basal planes of the hexagonal η' precipitates are partially coherent with the {111} matrix planes but the interface between the matrix and the c direction of the precipitate is incoherent. Aging times and temperatures that develop the highest strengths, characteristic of the T6 temper, produce zones having an average diameter of 2 to 3.5 nm (20 to 35 Å) along with some amount of η'. The nature of the zones is still uncertain, although they undoubtedly have high concentrations of zinc atoms and probably magnesium atoms as well. Some variation in x-ray and electron diffraction effects indicative of zone structure variations were noted, depending on relative zinc and magnesium contents of the alloys.

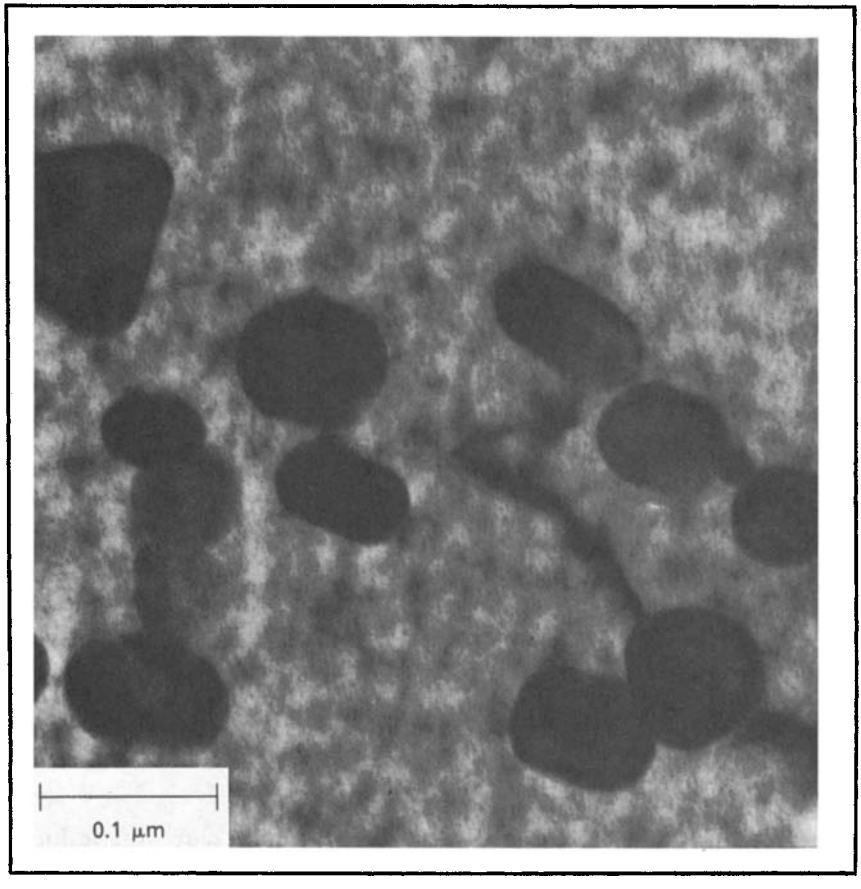

Fig. 7. Transmission electron micrograph of 7075-W aged 25 years at room temperature. The large particles are $Al_{12}Mg_2Cr$ dispersoid. The GP zones throughout the structure have an average diameter of 1.2 nm (12 Å), and an approximate density of 4×10^{18} zones per cm^{-3}. The yield strength of the as-quenched 7075-W was 150 MPa (22 ksi). After 25 years, yield strength had increased to 465 MPa (67 ksi).

Several investigators have observed that the transition phase η' forms over a considerable range of compositions that are in the Al + T field, as well as those in the Al + η field under equilibrium conditions (Fig. 8). With increased time or higher temperature, the η' converts to ($MgZn_2$) or, in cases where T is the equilibrium phase, is replaced by T ($Mg_3Zn_3Al_2$). Evidence exists for a transition form of T in alloys with lower zinc-magnesium ratios, at times and temperatures that produce overaging. The precipitation sequence depends on composition, but that of rapidly quenched material aged at elevated temperatures may be represented as:

$$\text{SS} \rightarrow \text{GP zones [spherical]} \begin{cases} \nearrow \eta' \rightarrow \eta \\ \searrow T' \rightarrow T \end{cases} \qquad \text{Eq 4}$$

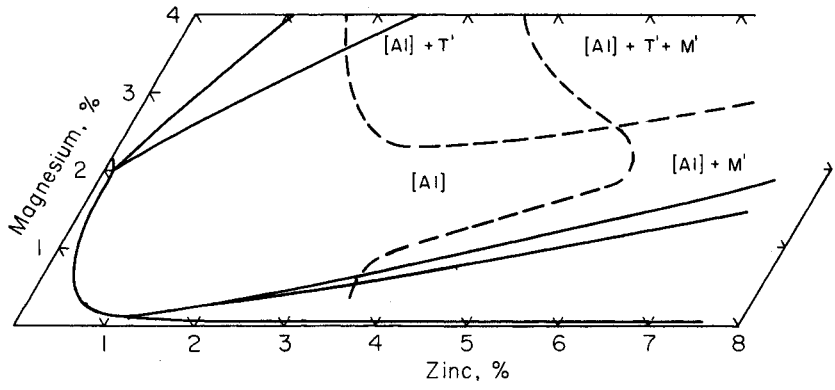

Fig. 8. Comparison of phases present in aluminum-magnesium-zinc alloys. Fields separated by dashed lines identify phases present after alloys were solution heat treated, quenched, and aged 24 h at 120 °C (250 °F) ([Al] = GP zone structure). Fields separated by solid lines are phases in equilibrium at 175 °C (350 °F). (H.C. Stumpf, Alcoa)

In this schematic, GP zones nucleate homogeneously, and the various precipitates develop sequentially within the matrix. However, the presence of high-angle grain boundaries, subgrain boundaries, and lattice dislocations alters the free energy such that significant heterogeneous nucleation may occur either during quenching or aging above a temperature known as the GP zone solvus temperature. Above this temperature, the semicoherent transition precipitates nucleate and grow directly on dislocations and subgrain boundaries, and the incoherent equilibrium precipitates nucleate and grow directly on high-angle boundaries. These heterogeneously nucleated precipitates do not contribute to strength and, hence, decrease attainable strength by decreasing the amount of solute available for homogeneous nucleation.

Decreasing the quench rate has another consequence besides allowing solute atoms an opportunity to nucleate heterogeneously. Slow quenching permits vacancies to migrate to free surfaces and become annihilated. Decreasing the number of vacancies decreases the temperature at which GP zones nucleate homogeneously. Therefore, a particular aging temperature may allow only homogeneous nucleation to occur in rapidly quenched materials, but may allow heterogeneous nucleation to predominate in slowly quenched material. Under the latter conditions, the precipitate distribution is extremely coarse, so strength developed is particularly low. Some of the loss in strength from slow quenching in this case can be minimized by decreasing the aging temperature to maximize homogeneous nucleation.

When an aged aluminum-zinc-magnesium alloy is exposed to a temperature higher than that to which it has previously been exposed, some GP zones dissolve while others grow. Whether a GP zone dissolves or grows depends on its size and on the exposure temperature. When the zone size is large enough, most of the zones transform to transition precipitates even above the GP zone solvus temperature. This phenomenon

is the basis for the two-step aging treatments to be discussed in a later section of this chapter.

The addition of up to 1% copper to the aluminum-zinc-magnesium alloys does not appear to alter the basic precipitation mechanism. In this range, the strengthening effects of copper are modest and attributed primarily to solid solution. Higher copper contents afford greater precipitation hardening, with some contribution of copper atoms to zone formation, as indicated by an increased temperature range of zone stability. Crystallographic arguments indicate that copper and aluminum atoms substitute for zinc in the $MgZn_2$ transition and equilibrium precipitates. In the quaternary aluminum-zinc-magnesium-copper system, the phases $MgZn_2$ and MgAlCu form an isomorphous series in which an aluminum atom and a copper atom substitute for two zinc atoms. Moreover, electropotential measurements and x-ray analyses indicate that copper atoms enter into the η' phase during aging temperatures above about 150 °C (300 °F). These observations are significant because aging aluminum-zinc-magnesium-copper alloys containing above about 1% copper above this temperature substantially increases their resistance to stress-corrosion cracking. Little effect is shown on the stress corrosion of alloys containing lower amounts of copper.

INGOT PREHEATING TREATMENTS

The initial thermal operation applied to ingots prior to hot working is referred to as "ingot preheating" or "homogenizing" and has one or more purposes depending on the alloy, product, and fabricating process involved. One of the principal objectives is improved workability. As described in Chapter 2 of this Volume, the microstructure of most alloys in the as-cast condition is quite heterogeneous. This is true for alloys that form solid solutions under equilibrium conditions and even for relatively dilute alloys. The cast microstructure is a cored dendritic structure with solute content increasing progressively from center to edge with an interdendritic distribution of second-phase particles or eutectic.

Because of the relatively low ductility of the intergranular and interdendritic networks of these second-phase particles, as-cast structures generally have inferior workability. The thermal treatments used to homogenize cast structures for improved workability were developed chiefly by empirical methods, correlated with optical metallographic examinations, to determine the time and temperature required to minimize coring and dissolve particles of the second phase. More recently, methods have become available to determine quantitatively the degree of microsegregation existing in cast structures and the rates of solution and homogenization. Figure 9 shows the microsegregation measured by an electron microprobe across the same dendrite cell in the as-cast condition and after the cell was homogenized by preheating. Rapid solidification, because it is quite different from equilibrium, produces maximum microsegregation across dendrite walls, and these cells are relatively small. The situation is complex, however, and in typical commercial ingots, large cells are more segregated than fine cells and, because diffusion distances are longer, large cells are more difficult to homogenize (Ref 12 and 13). For example, electron microprobe analyses of unidirectionally solidified cast-

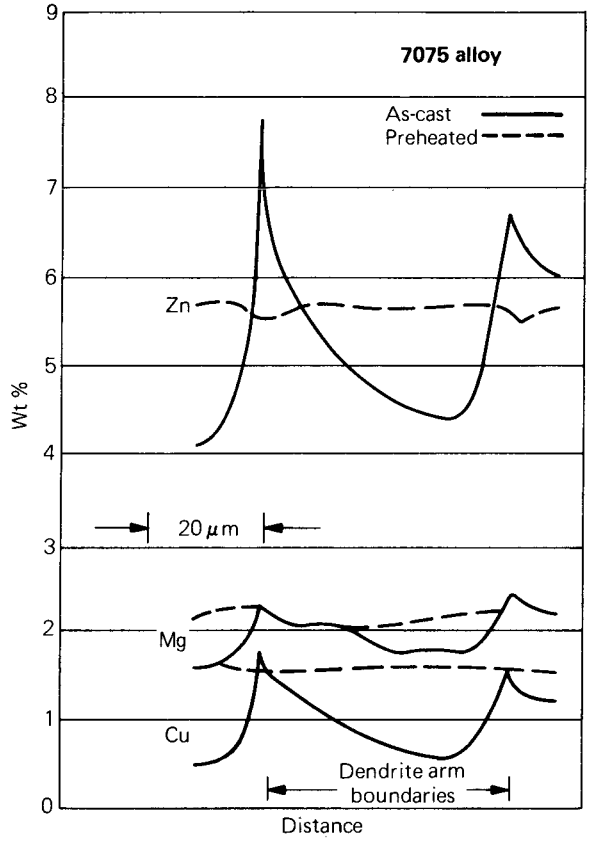

Fig. 9. Effect of preheating on ingot microsegregation.

ings of an Al-2.5% Mg alloy indicated that the degree of microsegregation was greater in the coarser, more slowly solidified structure, and that the approach to uniform solute distribution during heating at 425 °C (800 °F) was more rapid for the finer structure, as shown in Fig. 10.

Solution of the intermetallic phases rejected interdendritically during solidification, effected by the homogenizing operation, is only one step toward providing maximum workability. Because most of the solute is in solid solution after this heating, further softening and improvement in workability can be obtained by slow cooling, to re-precipitate and coalesce the solute in an intradendritic distribution of fairly large particles.

In aluminum-magnesium-silicon alloys, redistribution of magnesium and silicon occurs very rapidly, in as little as 30 min at 585 °C (1090 °F). However, greatly extended homogenizing periods result in a higher rate of extrusion and in an improved surface appearance of extruded products. The mechanism consists of spheroidizing the nearly insoluble iron-rich phases; the lower the solubility and diffusion rate of the elements involved, the slower the rate of spheroidization. Secondary effects are also achieved by precipitation of additional transition elements from solid so-

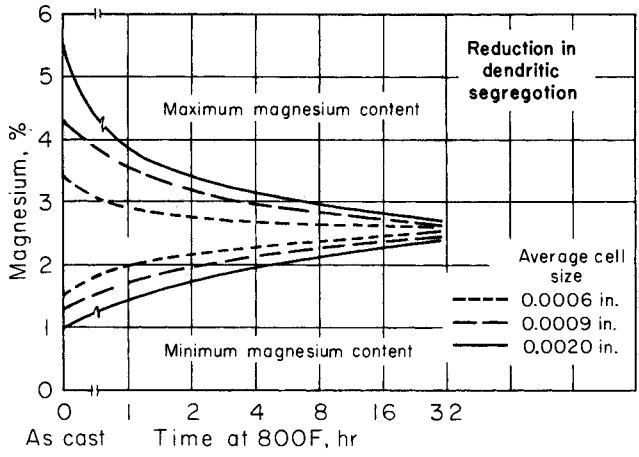

Fig. 10. Effect of time at 425 °C (800 °F) on maximum and minimum magnesium contents within dendrites of cast Al-2.5% Mg alloy. (W.G. Fricke, Jr., Alcoa Research Laboratories)

lution and by delayed peritectic transformations that could not go to completion during solidification.

Elements such as chromium and zirconium, which separate by a peritectic reaction during solidification, segregate in a manner just the reverse of that previously described. The first portion of the dendrite to solidify is richer in solute than the subsequently solidified portions. Consequently, the alloy content is maximum to the center of the dendrites and diminishes progressively toward the edges. The solid solutions formed by these elements and by manganese during rapid solidification are supersaturated with respect to their equilibrium solid solubilities. This is thought to result from the relatively low diffusion rates of the elements in the solid state.

Ingot preheating treatments for some of the alloys containing these elements are designed to induce precipitation, resulting in the formation of particles of equilibrium phases such as $Al_{20}Cu_2Mn_3$ and $Al_{12}Mg_2Cr$ with dimensions of 10 to 100 nm (1 to 10 Å). These high-temperature precipitates are frequently called dispersoids. They occur within the original dendrites, with a distribution essentially the same as that established during solidification, because the diffusion rates are too low to permit any substantial redistribution. In aluminum-magnesium-manganese alloys, the preheating operation increases the heterogeneity of manganese because of localized precipitation of manganese-bearing dispersoids near the dendrite arms. Nonuniform distribution persists in some wrought products, leading to microstructural patterns called banding. Ingot preheating treatments for certain alloys containing manganese, such as 3003, are designed to induce precipitation under controlled conditions; this lowers the recrystallization temperature and favors the development of fine, recrystallized grains during later process and final anneals (Ref 14).

Equilibrium Versus Nonequilibrium Melting. Figure 11 illustrates some of the restrictions that must apply to ingot preheating because of the phase diagram. The same principles apply to more complex systems,

but the details differ because different phases have different solvus temperatures and the eutectic may be a trough instead of a point.

Different compositions on the diagram represent different types of commercial alloys. Alloy X represents an alloy in which the alloy content does not exceed the maximum solubility. This is typified by relatively dilute alloys such as 2117, 6063, and 7029, but it is also true of alloys 7075 and 6061. Cursory examination of the phase diagram indicates that the ingot preheating range can be located anywhere between the solvus and solidus temperatures. However, to avoid the possibility of nonequilibrium melting, as explained below, either the upper limit should be below the eutectic temperature or the time below the eutectic temperature should be of sufficient duration to produce complete solution of the elements comprising the eutectic. Alloy Y represents an alloy in which an excess of soluble phase always remains undissolved. The upper end of the preheat temperature range must lie below the equilibrium eutectic temperature if melting is to be avoided. This case is typified by alloys 2219, 2011, and 7178. Alloys such as 2024 may respond like either alloy

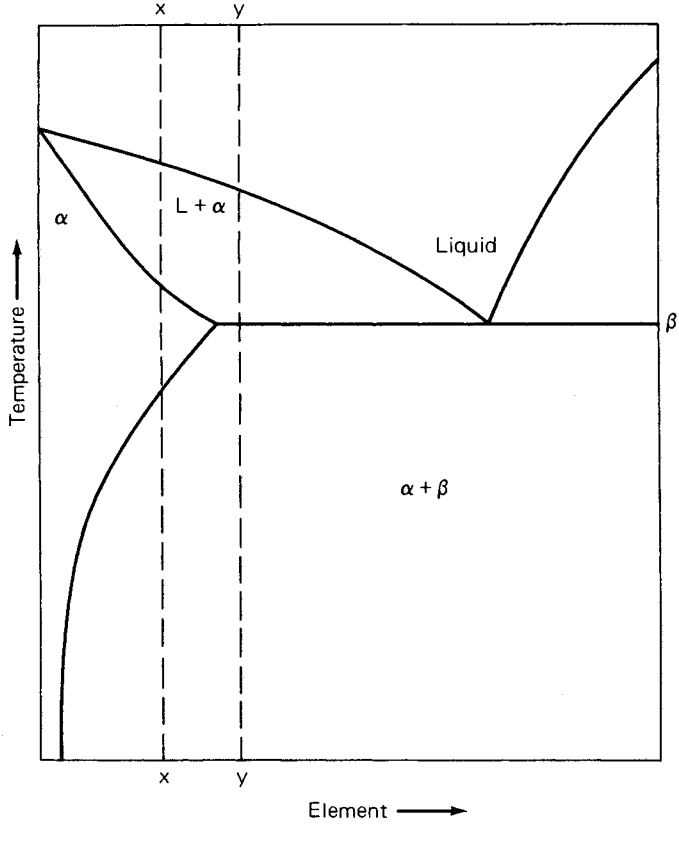

Fig. 11. Schematic phase diagram. Alloy X melts at the eutectic temperature if B is not dissolved below this temperature. Alloy Y always melts at the eutectic temperature.

X or alloy Y, depending on the amounts and proportions of the alloying and impurity elements.

Incipient melting, or the beginnings of liquid phase formation, can occur under either equilibrium or nonequilibrium conditions. Alloy Y in Fig. 11 obviously produces melting whenever its temperature is at or above the eutectic temperature. However, it is not as obvious that the same reaction occurs for alloy X, which has a higher equilibrium solidus temperature than alloy Y. When alloy X is in the as-cast condition, it contains a nonequilibrium eutectic structure. If reheating to the eutectic temperature is done at a rapid enough rate so that the soluble intermetallic cannot dissolve, the eutectic melts. Holding alloys like alloy X for sufficient time between the eutectic temperature and the true solidus causes the liquid phase to disappear as the soluble element passes into solution. The solution of the elements in the liquid phase leaves evidence in the form of microporosity at the previous sites of eutectic if the hydrogen content is above some critical level. The size of the micropores is smaller than the shrinkage porosity in good quality as-cast ingot. The principles expounded above apply to non-heat-treatable alloys as well as to heat treatable ones.

The real test of the harmfulness of overheating is whether there is microstructural damage of a type that cannot subsequently be repaired. Damage consists of excessive void formation, segregation, blistering, cracking, or severe external oxidation. Rosettes, the spherical structural feature that occurs when eutectic liquid solidifies during cooling after overheating, are very hard and persistent. They have been detected in thin sheet fabricated from thick, overheated ingot, despite extensive thermal-mechanical treatments used during the fabrication.

ANNEALING

Annealing may be required before forming or cold working heat treatable alloys, when they have been strain hardened by previous forming or are in heat treated tempers. The principles outlined in Chapter 4 of this Volume governing recovery, recrystallization, and grain size control for non-heat-treatable alloys apply also to the annealing of heat treatable alloys. However, the maximum temperature and cooling rate used must be more carefully controlled to avoid precipitation hardening either during or subsequent to annealing.

The type of annealing treatment required depends on the previous thermal and mechanical history, and the structure resulting from these prior operations. Alloys that are initially in the F temper may require annealing; O-temper material may require re-annealing after partial forming. Under these conditions, the operations that preceded forming already have caused the extensive precipitation and coalescence of precipitates that is desired, so that the objective of the annealing treatment is only to remove the strain hardening. This can be accomplished by heating to about 345 °C (650 °F) and holding long enough to ensure attainment of uniform temperature. The rates of heating and cooling are not critical in this operation, although a rapid heating rate is preferred to provide a fine grain size.

The annealing of alloys that have previously been heat treated to tem-

pers such as W, T3, T4, T6, or T8 requires use of treatments that first cause the precipitates to reach their equilibrium crystal structure and then cause them to coarsen. This can be accomplished by heating for 2 to 3 h at about 355 to 410 °C (675 to 775 °F) or slightly higher, followed by cooling to about 260 °C (500 °F) at rates of about 25 to 40 °C/h (45 to 72 °F/h). A too-slow cooling rate results in platelets of precipitate and poor formability in 7XXX alloy sheet. In the case of 2XXX series alloys, this treatment should precipitate most of the copper, leaving only 0.4 to 0.5% in solution. For 7XXX series alloys, even slow cooling does not provide sufficiently complete precipitation to remove solid solution effects and prevent natural aging; a period of additional heating at 230 °C (450 °F) for 2 to 6 h may be used to attain maximum stability and formability. Despite this more extensive procedure, the alloy annealed from the heat treated tempers usually has slightly poorer formability than annealed material not previously heat treated. In annealing thin-gage clad products, the heating time at the maximum temperature must be limited to avoid excessive diffusion from core to cladding. Annealing treatments are applied to castings only when the most exacting requirements for dimensional stability must be met, or when some unusual forming operation is specified.

SOLUTION HEAT TREATING

The purpose of solution heat treatment is to put the maximum practical amount of hardening solutes such as copper, magnesium, silicon, or zinc into solid solution in the aluminum matrix. For some alloys, the temperature at which the maximum amount is soluble corresponds to a eutectic temperature. Consequently, temperatures must be limited to a safe level below the maximum to avoid consequences of overheating and partial melting. Alloy 2014 exhibits this characteristic. Figure 12 illustrates

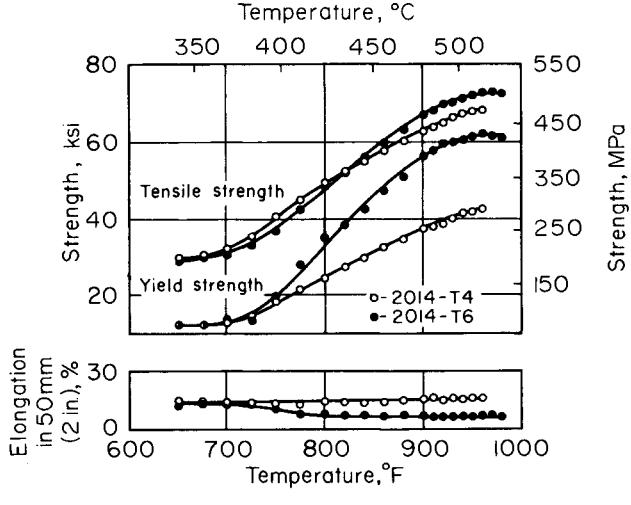

Fig. 12. Effects of solution heat treating temperature on the tensile properties of 2014-T4 and 2014-T6 sheet.

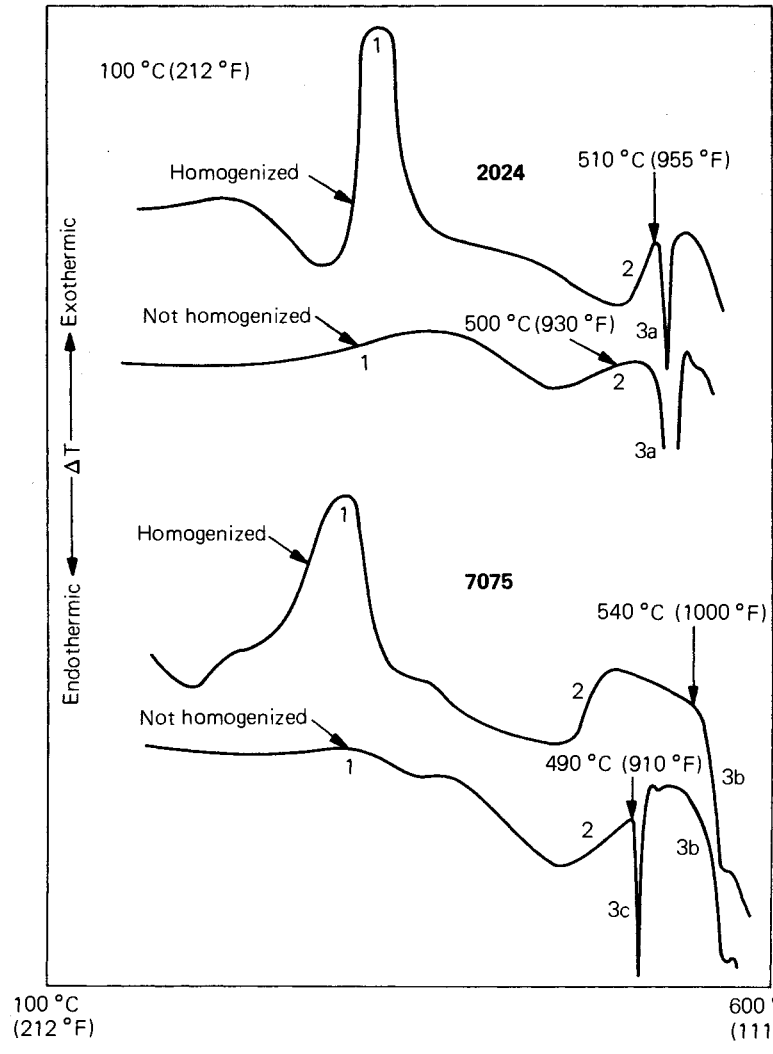

Fig. 13. DTA curves at 20 °C/min (36 °F/min) heating, indicating temperatures for easily identified beginning of melting (shown by arrows). Significant curve inflections are (1) precipitation from saturated solid solution, (2) re-solution of precipitated phase(s), and (3) melting. Equilibrium eutectic melting for 2024 is indicated by (3a); equilibrium solidus melting for 7075 by (3b), and nonequilibrium eutectic melting for 7075 by (3c).

the effect of solution temperature on the tensile properties of 2014-T4 and 2014-T6. Other alloys such as 7029 are more dilute with respect to their maximum solubility, and greater temperature tolerances are allowable. Nevertheless, the upper limit must be set with a regard to grain growth, surface effects, and economy of operation.

Some alloys, such as 7075 and 7050, which should allow much leeway in selection of solution temperature, based on the equilibrium solvus and

solidus temperature, can exhibit incipient melting at temperatures much below the latter under certain circumstances. Chapter 3 in this Volume shows that alloy 7075 has two soluble phases—$MgZn_2$ (with aluminum and copper substituting for some zinc) and Al_2CuMg. The latter phase is very slow to dissolve. Local concentrations of this phase can produce a nonequilibrium melting between 485 and 490 °C (905 and 910 °F) if brought to this or a higher temperature too rapidly. Figure 13 shows this by means of differential thermal analysis curves. A sample of nominal composition alloy 7075 that had been well homogenized and quenched began to melt somewhere in excess of 540 °C (1000 °F), while one not homogenized showed an endothermic spike indicating incipient melting at 490 °C (910 °F). Nominal composition 2024 cannot be homogenized to remove the S phase, and melting occurs near 510 °C (955 °F) in products that are homogenized and not homogenized. The curves indicate that only the quantity of liquid phase formed differed.

The grain size of heat treated aluminum alloys is greatly influenced by the amount of cold work introduced before the solution heat treatment. In general, grain size decreases as the amount of cold work prior to solution increases. With small amounts of cold work, usually less than 15%, grains may develop that are so coarse that relatively few are contained in the cross section of a standard tension test coupon. Although mechanical properties of heat treated aluminum alloys are generally insensitive to grain size, the properties are affected under these conditions. This phenomenon is illustrated in Fig. 14 for alloy 7475 sheet. Because of this effect of critical strain, care must be taken that parts formed from an

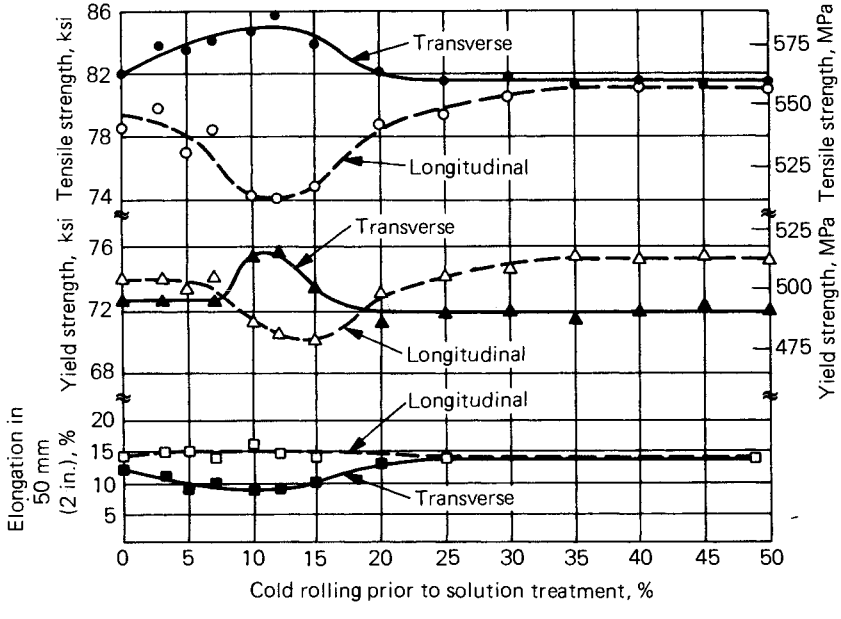

Fig. 14. Effect of cold work prior to solution treatment on tensile properties of 7475-T6 sheet.

annealed temper and subsequently heat treated have sufficient strain hardening at all locations.

For products that are annealed and cold worked prior to heat treatment, the annealing practice and the rate of heating to the solution heat treating temperature also affect grain size. Fine grain sizes are favored by annealing practices that give a copious distribution of coarse precipitates and by high heating rates. The coarse precipitates serve as nucleation sites for recrystallization, and the high heating rates ensure that nucleation begins before the precipitates dissolve. Air is the usual heating medium, but molten salt baths or fluidized beds are advantageous in providing more rapid heating.

The time required for solution heat treating depends on the type of product, alloy, casting or fabricating procedure used and thickness insofar as it influences preexisting microstructure. These factors establish the proportions of the solutes that are in or out of solution and the size and distribution of precipitated phases. Sand castings are usually held at the solution temperature for about 12 h; permanent mold castings, because of their finer structure, may require only 8 h. Thick-section wrought products are generally heated longer, the greater the section thickness. Once the product is at temperature, the rate of dissolution is the same for a given size of particle, regardless of section thickness. The main consideration is the coarseness of microstructure and the diffusion distances required to bring about a satisfactory degree of homogeneity. Thin products such as sheet may require only a few minutes. To avoid excessive diffusion, the time of solution heat treatment for clad sheet products must be limited to the minimum required to develop the specified mechanical properties. For the same reason, limitations are placed on reheat treatment of thin clad products where the correspondingly thin clad layer changes composition rapidly and loses its effectiveness in protecting against corrosion.

Reheat treating of previously heat treated products is subject to other hazards. When cold working has been applied after the previous heat treatment to develop T3 or T8 tempers, the residual strain may be of the critical amount to cause excessively large recrystallized grains. In reheat treating 2XXX series alloys, the temperature must not be lower than that of the original treatment, and heating time should be prolonged. Otherwise, corrosion resistance may be impaired and formability is seriously decreased by the development of continuous, heavy precipitate at grain boundaries.

A condition called "high-temperature oxidation" (HTO) or "high-temperature deterioration" results when metal is heated to solution heat treatment temperatures in a furnace that has too much moisture in the atmosphere. It is aggravated when the moist atmosphere is contaminated with gases containing sulfur. This condition manifests itself by formation of rounded voids or crevices within the metal and by surface blisters. It occurs when atomic hydrogen, formed when moisture reacts with the aluminum surfaces, diffuses through the aluminum lattice and recombines to form molecular hydrogen at locations of lattice discontinuity and disregistry. Such reactions may be alleviated by using moisture-free atmos-

pheres, or by use of volatile fluoride-containing salts or boron-trifluoride gas injected into the furnace atmosphere.

Severe void formation and blistering may also be a consequence of severe but temporary overheating. It may have the same aspect as high-temperature oxidation if, during the heat treatment cycle, the temperature is brought back down to the normal range and held before the metal is quenched. In this instance, the solute-enriched liquid phase disappears through resolidification and dissolution. Hydrogen undoubtedly plays a role, but the primary problem is partial melting. This phenomenon can be distinguished from high-temperature oxidation by the distribution of the voids; with HTO, the number of voids progressively decreases as distance from the surface increases. With this phenomenon, the voids are scattered throughout the workpiece.

Another phenomenon may also cause microvoid formation. The soluble phases containing magnesium have a tendency to leave behind microvoids when they dissolve, especially when the particles are large and the heating rate is very rapid. This has been attributed to a density difference between particle and matrix and insufficient time for aluminum atoms to back-diffuse into the volume formerly occupied by the particle. No known detrimental effect of these voids exists, unless they are combined with high-temperature oxidation.

QUENCHING

Quenching is in many ways the most critical step in the sequence of heat treating operations. The objective of quenching is to preserve the solid solution formed at the solution heat treating temperature, by rapidly cooling to some lower temperature, usually near room temperature. From the preceding general discussion, this statement applies not only to retaining solute atoms in solution, but also to maintaining a certain minumum number of vacant lattice sites to assist in promoting the low-temperature diffusion required for zone formation. The solute atoms that precipitate either on grain boundaries, dispersoids, or other particles, as well as the vacancies that migrate (with extreme rapidity) to disordered regions, are irretrievably lost for practical purposes and fail to contribute to the subsequent strengthening.

As a broad generalization, the highest strengths attainable and the best combinations of strength and toughness are those associated with the most rapid quenching rates. Resistance to corrosion and to stress-corrosion cracking are other characteristics that are generally improved by maximum rapidity of quenching. Some of the alloys used in artificially aged tempers and in particular the copper-free 7XXX alloys are exceptions to this rule. The argument for maximum quenching rate also is not entirely one-sided, because both the degree of warpage or distortion that occurs during quenching and the magnitude of residual stress that develops in the products tend to increase with the rate of cooling. In addition, the maximum attainable quench rate decreases as the thickness of the product increases. Because of these effects, much work has been done over the years to understand and predict how quenching conditions and product form influence properties.

Critical Temperature Range. The fundamentals involved in quenching precipitation-hardenable alloys are based on nucleation theory applied to diffusion-controlled solid-state reactions. The effects of temperature on the kinetics of isothermal precipitation depend principally upon the degree of supersaturation and the rate of diffusion. These factors vary oppositely with temperature, as illustrated in Fig. 15 for an alloy having a composition C_1 in a system with a solvus curve C_S. The degree of supersaturation after solution heat treating (C_1 - C_S) is represented by the curve S and the rate of diffusion by curve D. When either S or D is low, the rate of precipitation, represented by curve P, is low. At intermediate temperatures, both of the rate-controlling factors are favorable, and a high rate of precipitation may be expected.

Fink and Willey pioneered attempts to describe the effects of quenching on properties of aluminum alloys (Ref 15). Using isothermal quenching techniques, they developed C-curves for strength of 7075-T6 and corrosion behavior of 2024-T4. The C-curves were plots of the time required at different temperatures to precipitate a sufficient amount of solute to either reduce strength by a certain amount or cause a change in the corrosion behavior from pitting to intergranular. Inspection of the curves revealed the temperature range that gave the highest precipitation rates. Fink and Willey called this the critical temperature range.

Investigators used critical temperature ranges in conjunction with properties of samples quenched continuously from the solution temperature to compare relative sensitivities of alloys to quenching condition. Strength, as a function of quenching rate, was determined for a number of the commercial heat treatable aluminum alloys by quenching sheet and plate panels of various thicknesses in different media to produce a wide range of cooling rates through the critical temperature range. Representative tensile strength data for several alloys are presented in Fig. 16. The reduction in strength for a specific decrease in cooling rate differs from one

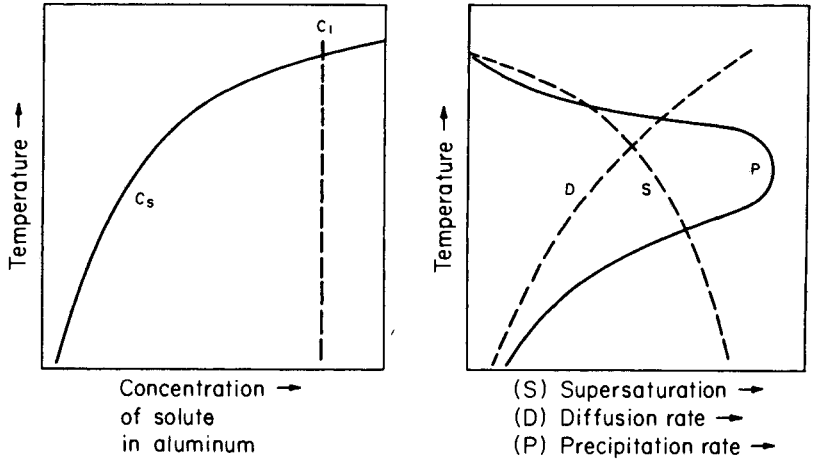

Fig. 15. Schematic representation of temperature effects on factors that determine precipitation rate.

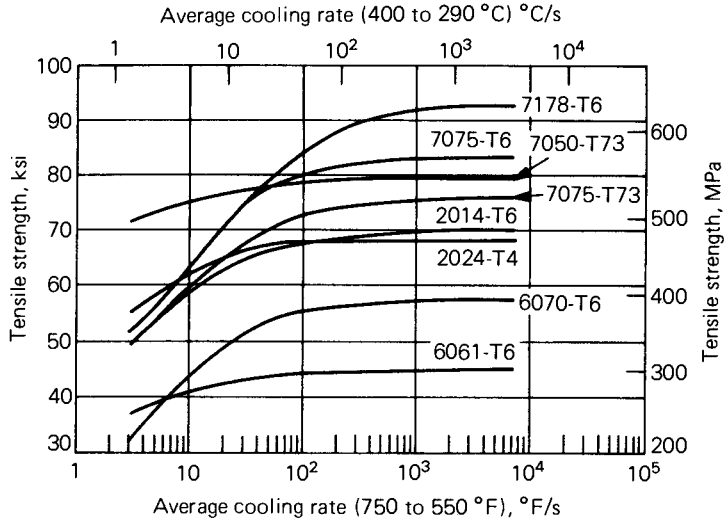

Fig. 16. Tensile strengths of eight alloys as a function of average cooling rate during quenching.

alloy composition to another. In comparing two alloys, the one having the higher strength in the form of sheet or a thin-walled extrusion may exhibit the lower strength when produced as a thick plate, extruded section, or forging. The relative strength rating of the alloys at a given cooling rate may also shift with temper. These factors may significantly influence the selection of alloy and temper for a specific application.

Quench Factor Analysis. Although useful as a first approximation, average quenching rates and critical temperature ranges are too qualitative to permit accurate prediction of the effects of quench rates when the rate of cooling does not change smoothly (Ref 16). To handle such instances, a procedure known as quench factor analysis has been developed. This procedure uses the information in the entire *C*-curve. Precipitation kinetics for continuous cooling are defined by the equation:

$$\xi = 1 - \exp(k\tau) \qquad \text{Eq 5}$$

where ξ is the fraction transformed and k is a constant, and:

$$\tau \int = \frac{dt}{C_t} \qquad \text{Eq 6}$$

where t is time and C_t is the critical time as a function of temperature (the loci of critical times is the *C*-curve.)

When $\tau = 1$, the fraction transformed, ξ, equals the fraction transformed designated by the *C*-curve. The solution of the integral, τ, has been designated the quench factor, and the method of using the *C*-curve and the quench curve to predict properties has been termed quench factor analysis. To perform quench factor analysis, the integral above is graphically evaluated to the required accuracy using the method shown in Fig. 17. Examples of ways to use quench factor analysis to predict corrosion resistance and yield strength are presented later in this chapter.

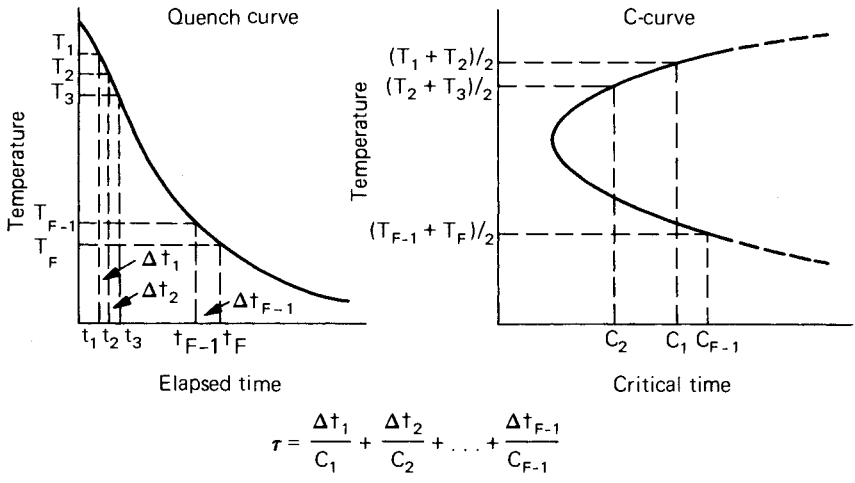

Fig. 17. Method of evaluating τ from the **C***-curve and a quench curve.*

Predicting Corrosion. Alloy 2024-T4 is susceptible to intergranular corrosion when a critical amount of solute precipitates during the quench, but corrodes in the less severe pitting mode when lesser amounts precipitate. To predict effects of proposed quenching conditions on corrosion characteristics of 2024-T4, the postulated quench curve is drawn, and the quench factor is calculated using the *C*-curve in Fig. 18. Corrosion characteristics are predicted from the plot in Fig. 19. When the quench factor, τ, is less than 1.0, the corrosion mode of continuously quenched 2024-T4 is pitting.

One application of these relationships is in studies of effects of proposed changes in quench practice on design of new quenching systems. For example, consider that a goal of a proposed quenching system for

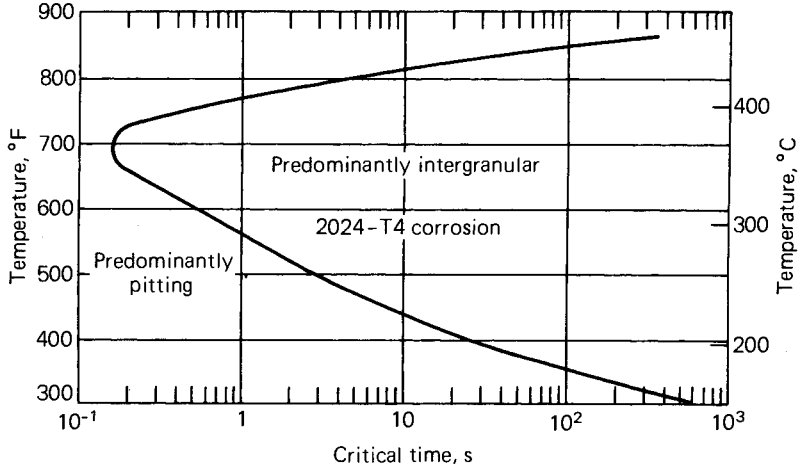

Fig. 18. **C***-curve for intergranular corrosion of 2024-T4.*

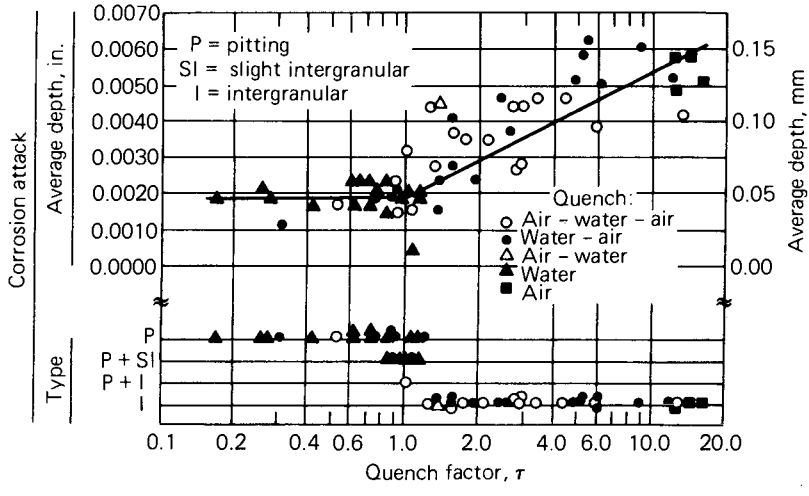

Fig. 19. Effect of quench factor on corrosion characteristics of 2024-T4.

alloy 2024-T4 sheet products is to minimize warping while preventing susceptibility to intergranular corrosion in sheet up to 3.2 mm (0.13 in.) thick. Warping occurs when stresses imposed by temperature differences across the sheet exceed the flow stress. These differences decrease as quench rate decreases, but the tendency toward intergranular corrosion increases. Quench factor analysis allows one to predict the effects on the corrosion mode of stepped quench practices to minimize warping.

As an example, one-step, two-step, and three-step quench curves that can provide acceptable corrosion characteristics in 3.2 mm (0.13 in.) 2024-T4 sheet (quench factor = 0.99) were calculated. Some of these are plotted in Fig. 20, which illustrates that 2024 can be quenched at a linear rate of 475 °C/s (855 °F/s), or higher. A quench rate below 150 °C (300 °F) was irrelevant. If the sheet is air-blast quenched with a rate of heat extraction of 5.68 W/m^2 per degree centigrade to 395 °C (740 °F), however, the quench rate from 395 to 150 °C (740 to 300 °F) must be at least 945 °C/s (1700 °F/s) to maintain the acceptable corrosion behavior. The sheet may also be quenched by a three-step practice of air blasting to 395 °C (740 °F), spray quenching at 3300 °C/s (6000 °F/s) to 245 °C (480 °F). The sheet is then air-blast quenched to 150 °C (300 °F). Other curves could be drawn, but the important points are that air-blast quenching cannot be continued more than a few degrees below 395 °C (740 °F), nor can it be initiated more than a few degrees above 270 °C (520 °F), even if infinite quench rates are attained from 395 to 270 °C.

Experimental quenching methods using continuous and various stepped quenching procedures were applied to verify that quench factor analysis could predict corrosion characteristics of 2024-T4. Figure 19 summarizes effects on type of corrosion attack observed with 2024-T4 sheet specimens quenched by these techniques. The results confirm that the method is valid for all types of quench paths evaluated and shows that corrosion depth increases progressively with increasing the quench factor above a value of 1.0.

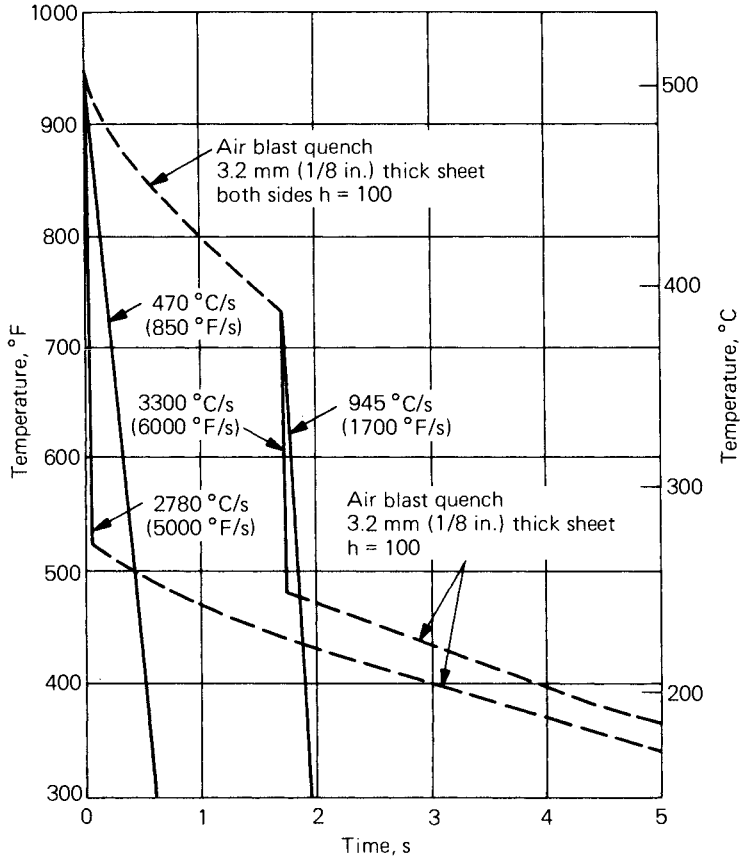

Fig. 20. Hypothetical cooling curves.

Predicting yield strength is more complex because knowledge of the relationship between the extent of precipitation and the ability to develop yield strength after aging is required. Attainable strength of 7XXX alloys is a function of the amount of solute remaining in solid solution after the quench, as long as aging is conducted so that GP zones nucleate prior to the appearance of η'. Under these conditions, relationships between the strength attainable after continuous cooling, σ, and quench factor, τ, can be represented by the following:

$$\sigma = \sigma_{max}\, \tau^{\exp(K)} \qquad \text{Eq 7}$$

where σ_{max} is the strength attainable with infinite quench rate and K is 0.005013 (natural log of 0.995) and

$$\tau = \int \frac{dt}{C_{99.5}} \qquad \text{Eq 8}$$

where t is time and $C_{99.5}$ is the C-curve for $\sigma_{99.5}$; critical time as a function of temperature to reduce attainable strength to 99.5% of σ_{max}.

The advantage of predicting yield strength from the quench factor instead of from the average quench rate is illustrated in the following com-

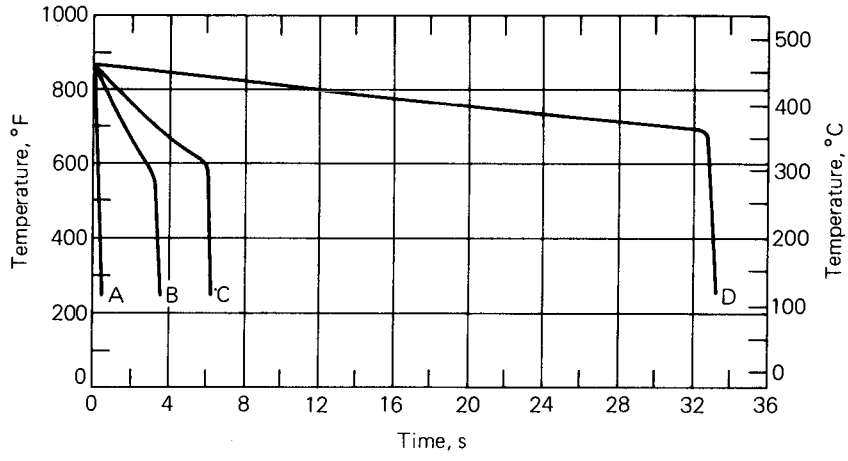

Quench	Average quench rate at 400-290 °C (750-550 °F) °C/s	°F/s	Quench factor, *f*	Measured yield strength MPa	ksi	Yield strength predicted from average quench rate MPa	ksi	Yield strength predicted from quench factor MPa	ksi
A, cold water	930	1680	0.464	506	73.4	499	72.4	498	72.3
B, denatured alcohol to 290 °C (550 °F), then cold water	49	88	8.539	476	69.1	463	67.2	478	69.4
C, boiling water to 315 °C (600 °F), then cold water	29	53	15.327	458	66.4	443	64.2	463	67.1
D, still air to 370 °C (700 °F), then cold water	5	9	21.334	468	67.9	242	35.1	449	65.1

Fig. 21. Cooling curves for 1.6-mm (0.06-in.) thick 7075 sheet.

parison. Four samples of 7075 quenched by various means (Fig. 21) were aged by the standard T6 practice of 24 h at 120 °C (250 °F). Yield strengths were predicted from both the average quench rate from 340 to 290 °C (750 to 550 °F) and from the quench factor. The quench factor was calculated using the *C*-curve for 99.5% maximum strength for 7075-T6 (Fig. 22), and yield strength was estimated from Eq 3 (graphically presented in Fig. 23).

A comparison of predicted yield strengths with actual yield strength is given in the table that accompanies Fig. 21. Yield strengths predicted from quench factors agree very well with measured yield strengths for all of the samples, the maximum error being 19.3 MPa (2.8 ksi). Yield strengths predicted from average quench rates, however, differ from the measured yield strength by as much as 226 MPa (32.8 ksi).

The advantage of using the quench factor for predicting yield strength from cooling curves is apparent. Average quench rate is not a predictor for cooling curves, which have long holding times either above or below the critical temperature range of 340 to 290 °C (645 to 555 °F), such as curve *D* of Fig. 21. For such cases, yield strength prediction using the quench factor is particularly advantageous.

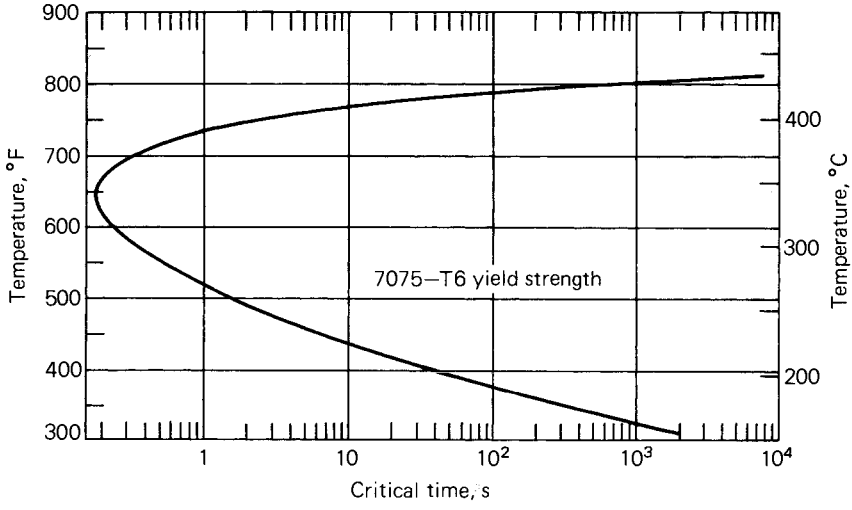

Fig. 22. **C-curve for 7075-T6 yield strength.**

Product Size and Shape. In commercial heat treating, the shape or dimensions of the product cannot be varied arbitrarily. Because heat transfer during quenching basically is limited by resistance at the surface in contact with the quenching medium, the rate of cooling is a function of the ratio of surface area to volume. This ratio may vary considerably, depending upon the shape of the product. For sheet and plate, as well as other products of similar shape, average cooling rates (through the critical temperature range measured at a center or midplane location) vary with thickness in a relatively simple manner. The relation can be approximated by the equation:

$$\text{Log } r_1 = \log r_2 - k \log t \qquad \text{Eq 9}$$

where r_1 is the average cooling rate at thickness t, r_2 is the average cooling rate at 1 cm (0.4 in.) thickness, and k is a constant.

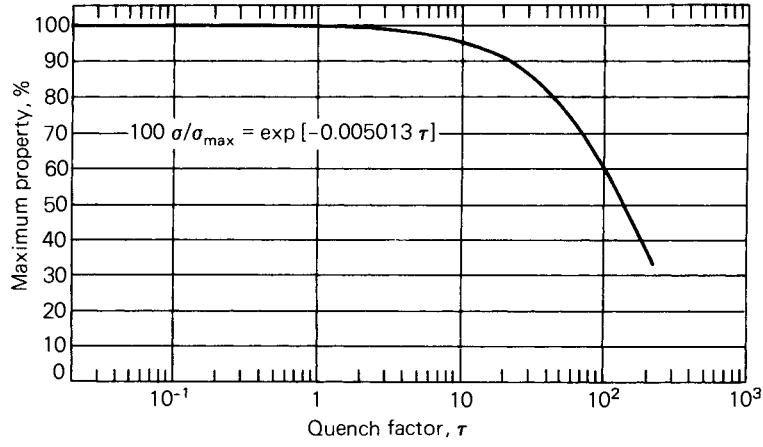

Fig. 23. Curve relating attainable strength to quench factor.

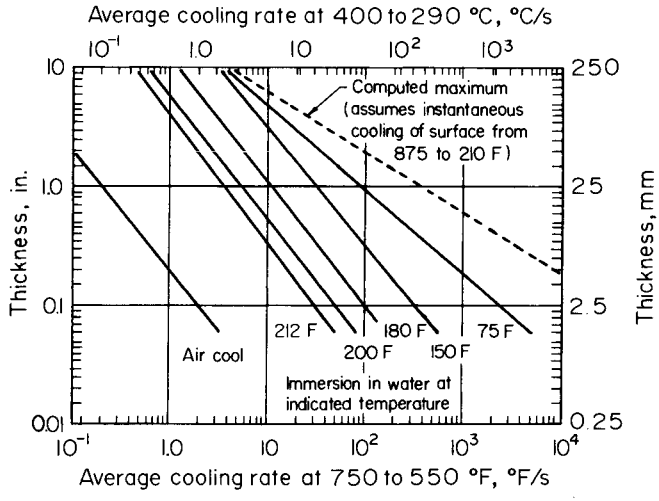

Fig. 24. Effects of thickness and quenching medium on average cooling rates at midplane of aluminum alloy sheet and plate quenched from solution temperatures.

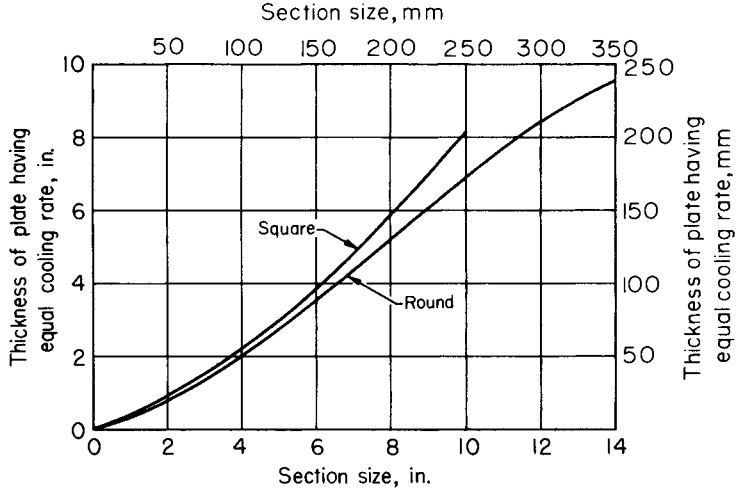

Fig. 25. Experimentally determined correlation between average cooling rates of 400 to 290 °C (750 to 550 °F) of rod and square bars to plates. Rates were measured at centers of sections.

Cooling rates determined experimentally for 1.6-mm (0.06-in.) to 20-cm (8-in.) thick sections that were quenched by immersion in water at five different temperatures and by cooling in still air are shown in Fig. 24. Experimentally determined relationships between the thickness of plates and either the diameter of rounds or the dimensions of square bars having equal cooling rates are shown in Fig. 25.

The dashed line at the extreme right in Fig. 24 delineates the maximum cooling rates theoretically obtainable at the midplane of plate, assuming an infinite surface heat transfer coefficient and a diffusivity factor of 1400

cm^2/s (Ref 17). No rates higher than those defined by this line have been observed, although rates approaching them were measured with impinging spray quenches. Because the rates indicated in Fig. 24 are for locations most distant from the surfaces, they are the lowest to be expected in sheet or plate. In plate, slightly higher rates should exist at the quarter-planes, and portions closer to the surface should cool at appreciably higher rates.

Quenching Medium. Water is the most widely used and most effective quenching medium. As Fig. 24 indicates, in immersion quenching, cooling rates can be reduced by increasing water temperature. Conditions that increase the stability of a vapor film around the part decrease the cooling rate; various additions to water that lower surface tension have the same effect. Slower cooling also results from the use of additions such as polyalkylene glycol that form film coatings on the hot metal. Organic quenching media provide lower cooling rates than water. Molten salt and low-melting eutectic baths have been used for experimental investigation of quench-aging treatments; these may have some advantage for continuous heat treatment of alloys that are adversely affected by a delay between quenching and aging (Ref 18). Moving air is sufficient for less quench-sensitive dilute alloys, such as 6063, when they are extruded in thin-walled sections.

Other Factors. Quenching rates are very sensitive to the surface condition of the parts. Lowest rates are observed with products having freshly machined or bright-etched, clean surfaces, or products that have been coated with materials that decrease heat transfer. The presence of oxide films or stains increases cooling rates. Further marked changes can be effected through the application of nonreflective coatings, which also accelerate heating, as shown in Fig. 26. Surface roughness exerts a similar effect; this appears related to vapor film stability. The manner in which complex products, such as engineered castings and die forgings, enter the quenching medium can significantly alter the relative cooling rates at various points, thereby affecting mechanical properties and residual stresses established during quenching. Similarly, quenching complex extruded

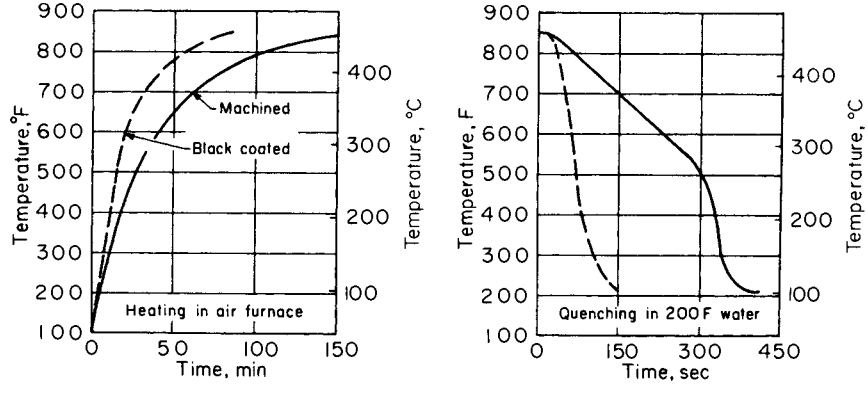

Fig. 26. Effect of surface condition on heating and cooling of 165-mm (6.5-in.) diam by 216-mm (8.5-in.) long aluminum alloy cylinder. Temperatures were measured at the center.

shapes whose wall thicknesses differ widely poses special problems if distortion and stresses are to be minimized. In batch heat treating operations, placement and spacing of parts on the racks can be a major factor in determining the quenching rates. In immersion quenching, adequate volumes of the quenching medium must be provided to prevent an excessive temperature rise in the medium. When jet agitation is used to induce water flow between parts, jets should not impinge directly and cause rapid localized cooling.

Reheating During Quenching. Recent information indicates that neither the average quenching rate through a critical temperature range nor quench factor analysis can predict strength when the temperature increases during quenching after it is cooled below some critical temperature (Ref 19 and 20). Under this condition, strength in the affected areas can be significantly lower than in other areas of the material. The most likely way for this phenomenon to occur is during spray quenching, when the surface cools rapidly by the impinging spray, but reheats by heat flow from the hotter interior when the spray is interrupted. Recent work may have explained the mechanism for the severe loss of strength in areas of alloy 2024 extrusions that were reheated under laboratory conditions (Ref 21). Nucleation is difficult during quenching, so few *S* or *S'* precipitates formed. It is postulated that, during reheating, many precipitates grew from the GP zones that nucleated homogeneously when the temperature fell below the GP zone solvus during the quench.

Predicting Strengths of Thick Products. Effects of the quenching rate on alloy strengths can be represented on a generalized graph of the type shown in Fig. 16, and the expected quenching rates of products having various shapes and dimensions can be determined from Fig. 24 and 25. Nevertheless, combining these two kinds of information to predict mechanical properties must be done with caution. Inconsistencies were encountered, for example, in correlating properties of thick sections quenched in high-cooling-rate media with properties of thinner sections quenched in media affording milder quenching action. One of the reasons for the inconsistencies is believed to be the different shapes of the cooling curves. This difficulty can be overcome by using quench factor analysis. The other reason is that the degree of recrystallization and texture of the thick and thin sections may be different.

Careful analyses were made of data from a large number of production-control tensile tests of bulk-quenched rolled, forged, and extruded products that varied in section thickness to a maximum of about 20 cm (8 in.). The tensile and yield strengths decreased with increasing section thickness over 2.5 cm (1 in.) in a simple linear relationship. This is illustrated by the average properties for 7075-T651 plate in Fig. 27. The reversal in curve direction at thicknesses lower than 2.5 cm (1 in.) is accounted for by a change in structure, from completely unrecrystallized to partially recrystallized. When test specimens of uniform size (2.5 cm^2 or 0.4 $in.^2$, or less) cut from products thicker than 2.5 cm (1 in.) were reheat treated, the tensile properties showed no consistent variation with product thickness. This indicates that the quenching rate is the major factor establishing the property differences of sections thicker than about 2.5 cm (1 in.).

Corrosion Resistance. Rates of cooling from the solution temperature

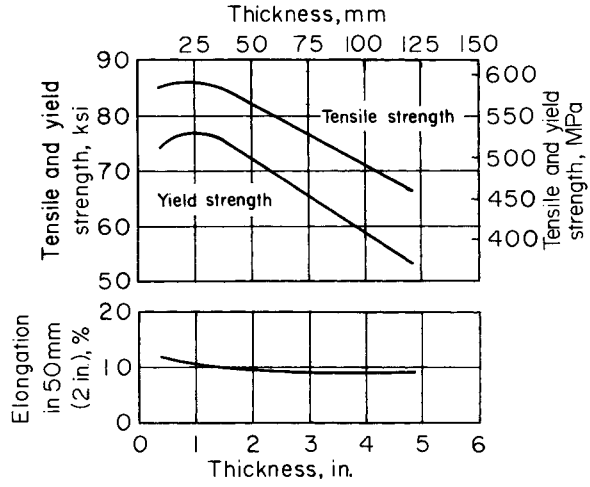

Fig. 27. Average tensile properties of 7075-T651 plate as a function of thickness.

markedly influence both the resistance of heat treatable alloys to corrosion and the characteristics of the corrosion attack. Extensive research with 7075-T6 sheet has shown that the material is subject only to pitting attack and has a high degree of resistance to stress corrosion and exfoliation if sufficiently rapid cooling is achieved during quenching. Conversely, when the cooling rate is relatively low, this alloy becomes prone to intergranular attack and may be susceptible to stress-corrosion cracking and exfoliation.

Experimental quenching methods, of the same type used to determine the critical temperature range that is important in developing strength, were applied to define the range in which the corrosion characteristics of 7075-T6 are established. The most critical changes occur in a similar temperature range for both corrosion characteristics and tensile properties. In Fig. 28, tensile strengths, losses in tensile strength after 12 weeks of alternate immersion in 3.5% NaCl solution, and the type and maximum depth of corrosion in NaCl-H_2O_2 solution (MIL-H-6088) are correlated with the average cooling rates through the critical temperature range. The most rapid decrease in tensile properties occurs at cooling rates somewhat higher than those that have the greatest effects on corrosion. To avoid completely the intergranular type of attack, rates in excess of about 165 °C/s (300 °F/s) are needed. Such rates are not attainable with thick sections. Therefore, when thick-section parts are required to endure service conditions conducive to stress corrosion in the short-transverse direction, the stress corrosion-resistance T73 temper of 7075 is preferred (Ref 22). When stresses in the short-transverse direction are low, but a resistance to exfoliation corrosion is required, 7075-T76 with strength intermediate to that of 7075-T6 and 7075-T73 is often specified. Newer alloys such as 7049-T73 and 7050-T74 develop superior combinations of strength and resistance to stress-corrosion cracking, particularly in thicker sections.

Delay in Quenching. The effects of delay in the transfer of parts from the solution heat treating furnace to the quenching medium are similar to those indicated for a reduction in the average cooling rate. Because the

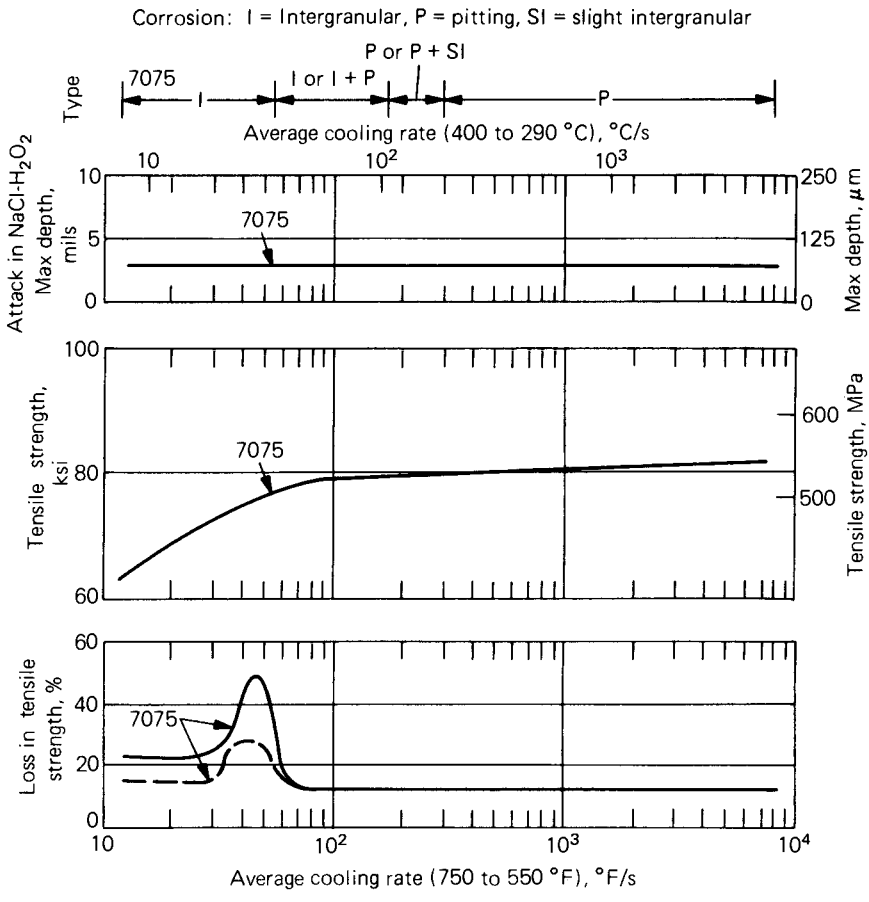

Fig. 28. Effects of quenching rate on tensile properties and corrosion resistance of 7075-T6 sheet. (B.W. Lifka and D.O. Sprowls, Alcoa Research Laboratories)

rate of cooling in air during the transfer is highly dependent upon the mass, section thickness, and spacing of the parts—and to a smaller extent upon air temperature, velocity, and emissivity—the allowable transfer time, or quench delay, varies with these factors. Certain specifications stipulate maximum delay periods ranging from 5 to 15 s for sheet under 0.4 mm (0.02 in.) to over 2.0 mm (0.08 in.) thick. Quench factor analysis indicates that the maximum allowable delay is also a function of the subsequent quenching conditions. Shorter times are required when the quench is less drastic than that obtained by a quench into cold water.

Fracture Toughness. As indicated previously, precipitation during the quench occurs initially on sites such as high-angle grain boundaries. The grain boundary precipitates and the associated precipitate-free zone that appears after aging provide a preferential fracture path. Consequently, decreasing the quench rate usually increases the proportion of intergranular fracture and decreases the fracture toughness of high-solute alloys, particularly those in T6-type tempers. The phenomenon cannot be reliably detected by the usual quality control tensile test because yield, ultimate,

and elongation values are usually not affected despite the low-energy, intergranular fracture mode. Tests of a specimen containing either a sharp notch or a crack must be used. The results of tear tests of alloy 7075-T6 sheet quenched in either cold or hot water, illustrated in Fig. 29, show how toughness can decrease significantly with an insignificant loss in strength. With extended precipitation within the grains, either as a result of a further decrease in the quench rate or overaging, strength begins to suffer. When the strength decrease gets large enough, toughness begins to increase (Fig. 30). The combination of strength and toughness, however, is highest in rapidly quenched material aged to peak strength.

Aluminum-magnesium-silicon alloys, although generally not considered for critical applications with fracture toughness requirements, can also suffer a loss in toughness and ductility in T6 and T5 tempers when the quench rate is low enough to permit substantial grain boundary precipitation. This is especially true when the silicon content is in excess of that required to form Mg_2Si and when elements that inhibit recrystallization are not present. In extreme cases, tensile fractures are completely intergranular.

Residual stresses originate from the temperature gradient produced by quenching. The gradient induces plastic deformation from differential contraction or expansion in the part (Ref 23 and 24). Because the surface of the part cools first, it tends to contract, thereby imposing a state of compressive stress on the interior. The reaction places the surface in tension. The surface layer deforms plastically when the tensile stress exceeds

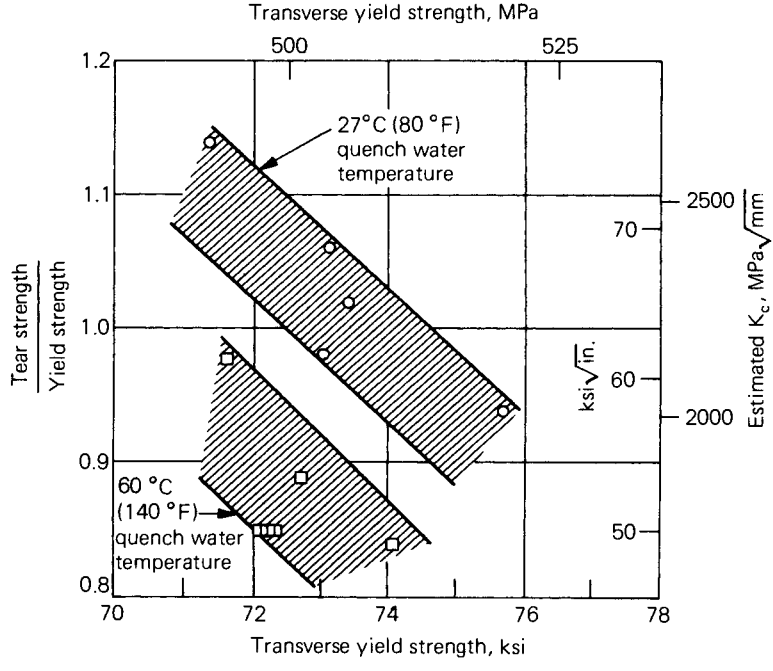

Fig. 29. Effects of quench water temperature on the tear strength and yield strength ratio of 7075 sheet.

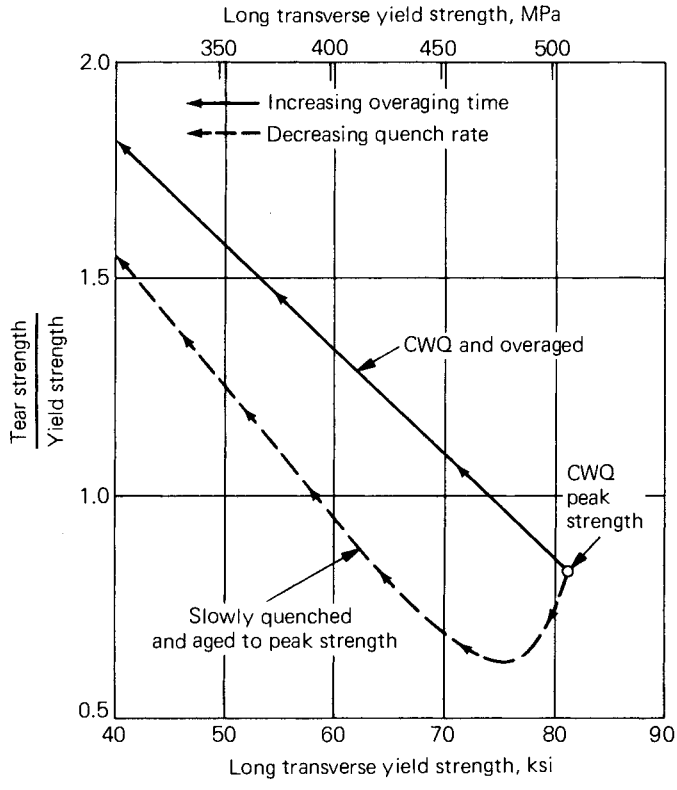

Fig. 30. Effects of quenching and aging condition on the tear strength and yield strength ratio of 7050 sheet.

the flow stress of the material. Then, as the interior of the part cools, it is restrained from contracting by the cold surface material. The resulting reaction places the surface in a state of compressive stress and the center in a state of tensile stress. When the part is completely cooled, it remains in a state of equilibrium, with the surface under high compression stresses balanced by tensile stresses in the interior. Generally, the compressive stresses in the surface layers of a solid cylinder are two-dimensional (longitudinal and tangential), and the tensile stresses in the core are triaxial (longitudinal, tangential, and radial), as illustrated in Fig. 31.

The magnitude of the residual stresses is directly related to the temperature gradients generated during quenching. Conditions that decrease the temperature gradient reduce the residual stress ranges (Ref 25). Quenching variables that affect the temperature gradient include the temperature at which quenching begins, cooling rate, section size, and variation in section size for nonflat products. For a part of a specific shape or thickness, lowering the temperature from which the part is quenched or decreasing the cooling rate reduces the magnitude of residual stress by reducing the temperature gradient. Figures 32 and 33 illustrate the effect of quenching temperature and cooling rate, respectively. With a specific

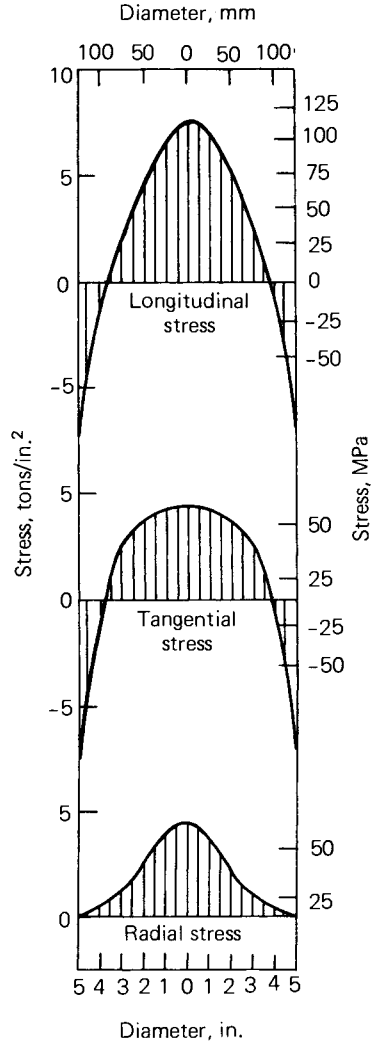

Fig. 31. Residual stress diagram for 2014 alloy quenched in cold water from 500 °C (935 °F).

cooling rate, the temperature gradient is greater in a section of large diameter or thickness than it is in a smaller section. Therefore, the residual stresses in the larger section are higher (Fig. 34). In products having differences in cross section, large temperature gradients can be minimized by covering or coating the thinner sections with a material that decreases the quench rate, so that it more closely matches that of the thicker sections.

The range of residual stresses generated during quenching varies considerably for different alloys. Those properties related to alloy composition that specifically affect the thermal gradient and the degree of plastic deformation that occur during quenching are involved. High residual stresses are promoted by high values of properties such as Young's modulus of

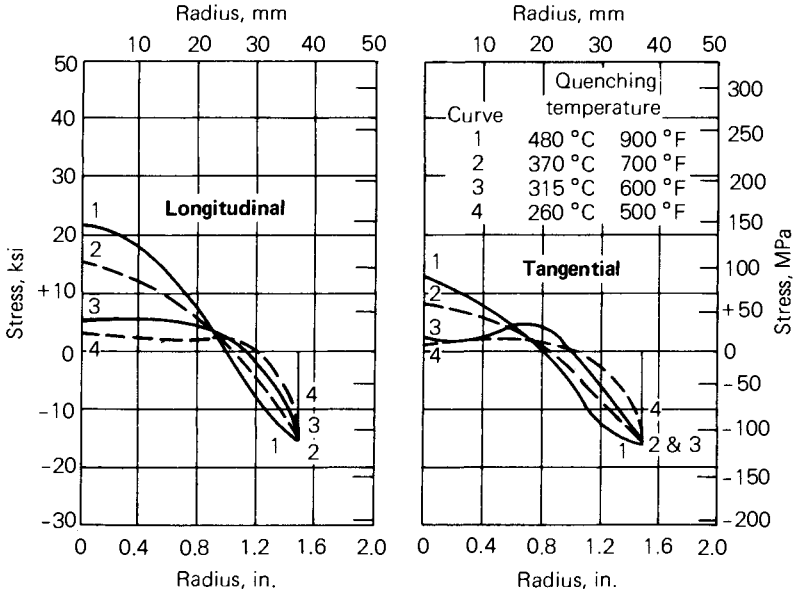

Fig. 32. Effect of quenching temperature on residual stresses in 5056 alloy cylinders of 76 by 229 mm (3 by 9 in.) quenched in water at 24 °C (76 °F).

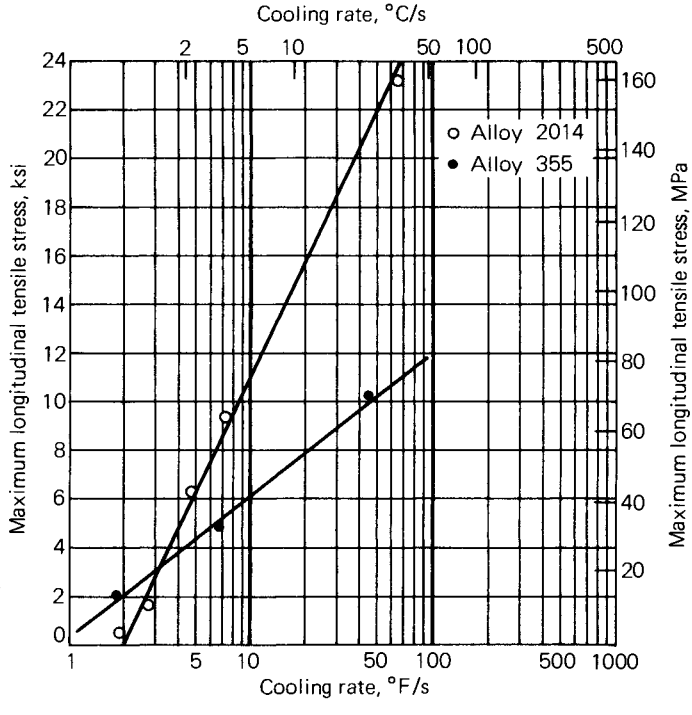

Fig. 33. Effect of quenching rate on residual stresses in 2014 and 355 alloy cylinders of 76 by 229 mm (3 by 9 in.) quenched from 500 °C (935 °F) and 525 °C (980 °F), respectively.

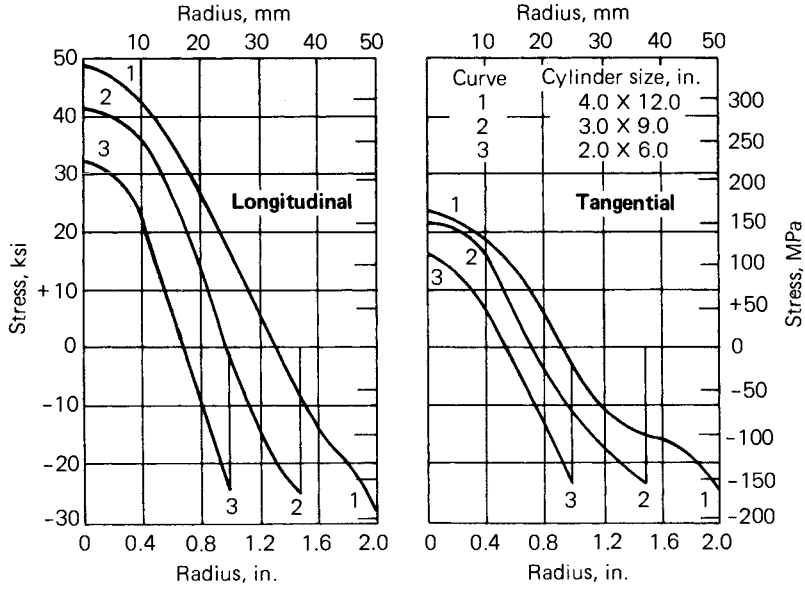

Fig. 34. Effect of section size on residual stresses in 2014 alloy cylinders quenched from 505 °C (940 °F) in water at 20 °C (70 °F).

elasticity, proportional limit at room and elevated temperature, and coefficient of thermal expansion; and by a low value of thermal diffusivity. These property factors affect the magnitude of residual stresses to different degrees. The influences of the coefficient of thermal expansion and elevated-temperature yield strength are especially significant. For example, a low coefficient of thermal expansion can counteract a high proportional limit. The net effect is a low residual stress level. Or, an alloy such as 2014 can develop a high residual stress range because of its very high elevated-temperature strength, despite average values for coefficient of thermal expansion, modulus of elasticity, and thermal diffusivity.

The effects of residual stresses from quenching require consideration in the application of heat treated parts. Where the parts are not machined, the residual compressive stresses at the surface may be favorable by lessening the possibility of stress corrosion or initiation of fatigue. However, heat treated parts are most often machined. Where the quenching stresses are unrelieved, they can result in undesirable distortion or dimensional change during machining. Metal removal upsets the balance of the residual stresses and the new system of stresses that restore balance generally results in warpage of the part. Further, in the final balance stress system, the machined surfaces of the finished part can be under tensile stress with attendant higher risk of stress corrosion or fatigue.

Because of the practical significance of residual stress in the application of heat treated parts, various methods have been developed either to minimize the residual stresses generated during quenching or to relieve them after quenching. The methods commonly used for stress relieving heat treated parts include mechanical and thermal methods. The methods used

to avert the development of high residual stresses during quenching rely on a reduced cooling rate to minimize the temperature gradients. Using quenching media that provide less rapid cooling in quenching irregularly shaped parts that cannot readily be stress relieved by subsequnt cold deformation is common practice. For this reason, the quenching of die forgings and castings in hot (60 to 80 °C or 140 to 180 °F) or boiling water is standard practice. In some cases, though, quench-rate sensitive alloys may suffer a loss in mechanical properties, particularly strength and fracture toughness. Intergranular corrosion resistance may also be impaired with such reduced cooling rates. Liquid organic polymer, such as polyalkylene glycol (10 to 40 vol% in water), is effective as a quenchant for minimizing residual stresses and distortion with lesser loss in properties (Ref 26-28). Owing to inverse solubility, a film of the liquid organic polymer is immediately deposited on the surface of the hot part when it is immersed in the quenchant. By reducing the rate of heat transfer, the deposited film reduces thermal gradients. Other additions to water, including suspensions of mineral powders, have been proposed. Extruded or rolled shapes may be cooled in an air blast, fog, or water spray. Production economics frequently favors the use of these milder quenches to decrease the need for straightening operations or to simplify machining operations because of the lower stresses. In other cases, the reduction in tension stress at machined surfaces of the finished part is most advantageous. In the manufacture of large, complex parts from die or hand forgings, an established practice is to heat treat after rough machining, thus averting the higher stresses that are associated with heat treating before metal removal.

Because of the trade-offs of tensile properties with residual stress, researchers have been developing methods of analysis that combine prediction of properties by quench factor analysis and prediction of stresses from heat transfer analyses and other considerations. One of these methods predicts that a cooling rate that is slow at the beginning, but continuously accelerates, can significantly reduce residual stresses while maintaining the same mechanical properties as those obtained by quenching in cold water (Ref 29). Another method, to eliminate warping of parts that have variations in section thickness without sacrificing mechanical properties, has been patented (Ref 30).

AGING AT ROOM TEMPERATURE (NATURAL AGING)

Most of the heat treatable alloys exhibit age hardening at room temperature after quenching. The rate and extent of such hardening varies from one alloy to another. Microstructural changes accompanying room temperature aging, except for long-time aging of 7XXX alloys, are undetectable because the hardening effects are attributable solely to the formation of zone structure within the solid solution. The changes in tensile properties for three representative commercial alloys aged at room temperature, 0 °C (32 °F), and −18 °C (0 °F) are shown in Fig. 35. In alloys 2024 and 2036, most of the strengthening occurs within a day at room temperature; the mechanical properties are essentally stable after four days. These alloys are widely used in the naturally aged tempers: T4, T3, and T361 for 2024 and T4 for 2036. Alloys 6061, 6009, and 6010 age more

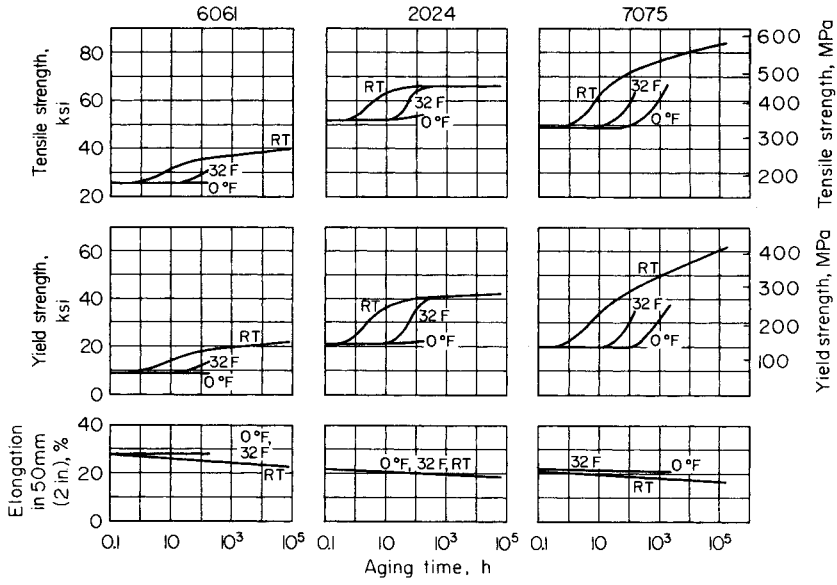

Fig. 35. Aging characteristics of aluminum sheet alloys at room temperature, 0 °C (32 °F), and −18 °C (0 °F). (J.A. Nock, Jr., Alcoa Research Laboratories)

slowly. Alloy 6061 may be used in the T4 temper; however, it is more frequently given a precipitation heat treatment to the T6 temper. Alloys 6009 and 6010, on the other hand, are commonly used in the T4 temper. However, these alloys are commonly used in automotive application, where paint baking is typically used. Consequently, they realize significant increases in strength during this thermal cycle, which is equivalent to an artificial aging treatment. Alloy 7075 and other 7XXX series alloys continue to age harden indefinitely at room temperature; because of this instability, they are very seldom used in the W temper.

Because heat treatable alloys are softer and more ductile immediately after quenching than after aging, straightening or forming operations may be performed more readily in the freshly quenched condition. For many alloys, production schedules must permit these operations before appreciable natural aging occurs. As alternatives, the parts may be stored under refrigeration to retard aging (Fig. 35), or they may be restored to near-freshly quenched condition by reversion treatments that dissolve the GP zones. The newer automotive body sheet alloys, however, remain highly formable even after extended natural aging. The introduction of localized strain hardening and residual stresses in parts by forming after quenching may have an adverse effect on fatigue, or on resistance to stress corrosion. In critical applications, forming prior to heat treatment is the procedure preferred to avoid these effects. In some cases, forming is permissible in the freshly quenched condition, but not after aging has occurred.

The electrical and thermal conductivities of most heat treatable alloys decrease with the progress of natural aging. This is in sharp contrast to the changes that occur during elevated-temperature aging. Electrical con-

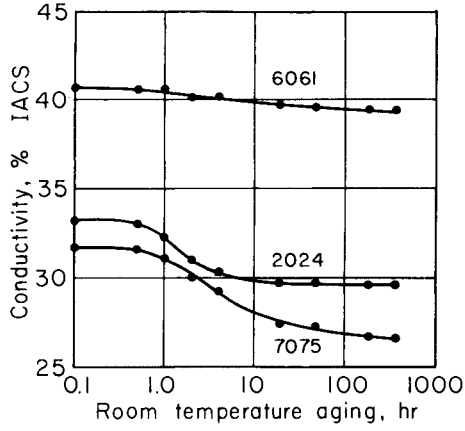

Fig. 36. Effects of room temperature aging on the electrical conductivity of as-quenched aluminum alloy sheet.

ductivity data for three alloys representing the major alloy types are presented in Fig. 36. Because a reduction of solid solution solute content normally increases electrical and thermal conductivities, the observed decreases are regarded as significant evidence that natural aging is a process of zone formation, not true precipitation. Decreased conductivity has been attributed to impairment of the periodicity of the lattice.

Castings are used in the naturally aged T4 temper in a relatively few instances where the higher ductility of this temper is of value. Hardening occurs with time after quenching, the rates varying considerably with alloy composition. The aluminum-magnesium alloy 220, normally used in the T4 temper, shows very gradual increases in strength over a period of years. The aluminum-zinc-magnesium casting alloys, which are used without heat treatment, exhibit a relatively rapid change in mechanical properties during the first three or four weeks at room temperature and subsequent additional aging at progressively reduced rates. In these alloys, a sufficient concentration of solute is retained in solution by the rate of cooling in the mold after solidification to permit substantial increases in strength.

PRECIPITATION HEAT TREATING (ARTIFICIAL AGING)

The effect of precipitation on mechanical properties is greatly accelerated, and usually accentuated, by reheating the quenched material to about 95 to 205 °C (200 to 400 °F). The effects are not attributable solely to a changed reaction rate; as mentioned previously, the structural changes occurring at the elevated temperatures differ in fundamental ways from those occurring at room temperature. These differences are reflected in the mechanical characteristics and some physical properties. A characteristic feature of elevated-temperature aging effects on tensile properties is that the increase in yield strength is more pronounced than the increase in tensile strength. Also, ductility and toughness decrease. Thus, an alloy in the T6 temper has higher strength but lower ductility than the same

alloy in the T4 temper. Overaging decreases both the tensile and yield strengths, but ductility generally is not recovered in proportion to the reduction in strengths, so that the combinations of these properties developed by overaging are considered inferior to those prevalent in the T6 temper or underaged conditions. Other factors, however, may greatly favor the use of an overaged temper. In certain applications, for example, strength factors are outweighed as criteria for temper selection by the resistance to stress-corrosion cracking, which improves markedly with overaging for some alloys, or by the greater dimensional stability for elevated-temperature service that is provided by overaging. In corrosive environments, resistance to the growth of fatigue cracks under constant amplitude and under various spectrum loading conditions increases with an increasing degree of overaging of 7XXX alloys. This improvement was a major factor influencing the decision to use 7475-T73 in a recent application in a fighter aircraft.

Precipitation-hardening curves (isothermal-aging curves) showing changes in tensile properties with time at constant temperature have been established for most of the commercial alloys at several temperatures and over extended periods of aging. To illustrate basic relationships, such data are summarized for alloys 2014 (aluminum-copper-magnesium-silicon) and 6061 (aluminum-magnesium-silicon) in Fig. 37. With both alloys, the curves reflect the influence of reversion, as shown by initial losses in strength. This initial softening is caused by partial destruction of the zone hardening prior to rehardening by precipitation. As mentioned previously, a special treatment based on the reversion phenomenon is occasionally

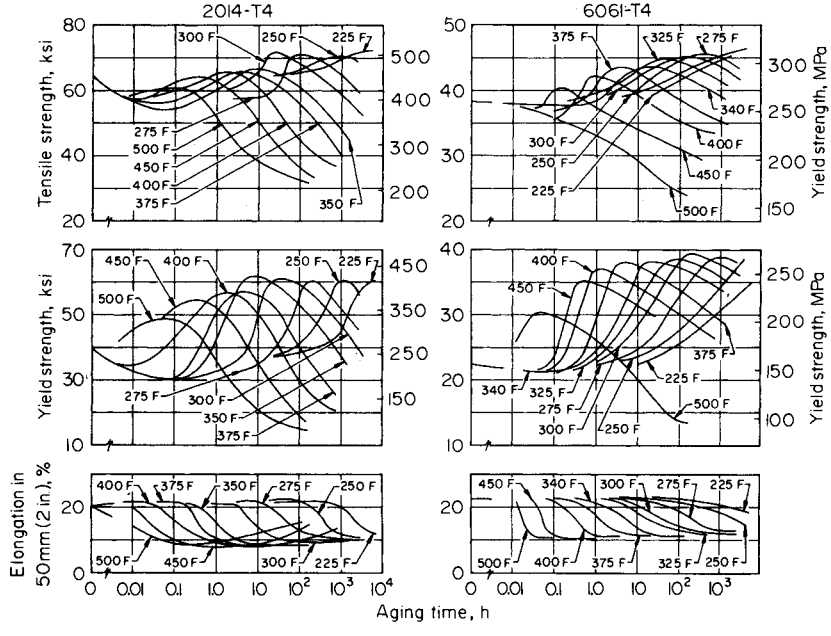

Fig. 37. Aging characteristics of two aluminum sheet alloys at elevated temperatures. (J.A. Nock, Jr., Alcoa Research Laboratories)

used to assist in forming alloys in the W or T4 temper. By heating the naturally aged alloy for a few minutes at temperatures in the artificial-aging range, the workability characteristic of the freshly quenched condition is restored. The effects are temporary, and the alloy re-ages at room temperature. Because such treatments decrease the corrosion resistance of series 2XXX alloys, they should be followed by artificial aging to obtain satisfactory corrosion characteristics.

The precipitation-hardening temperature range is similar for alloys 2014 and 6061, although aging is more rapid in 2014 at specific temperatures. Recommended commercial treatments for the T6 temper have been selected on the basis of experience with many production lots, representing an optimum compromise for high strengths, good production control, and operating economy. These consist of 8 to 12 h at 170 °C (340 °F) for 2014, and 16 to 20 h at 160 °C (320 °F) or 6 to 10 h at 175 °C (350 °F) for 6061, depending on product form.

Some paint bake operations are in the temperature range commonly used to artificially age. Consequently, auto body sheet can be formed in the T4 temper where formability is high, and then it can be aged to higher strengths during the paint bake cycle. Alloy 6010 was developed to maximize the response to aging in the temperature range used for paint baking. The differing behavior of alloys 6010 and 2036 in this respect are illustrated by the isostrength curves in Fig. 38 and 39.

Aging practice and cold work after quenching affect the combinations of strength and ductility or toughness that are developed. The curves of Fig. 37 illustrate the fact that recovery of ductility in the overaged condition is not appreciable until severe reduction in strength is encountered. The relationship between strength and toughness of notched specimens of two alloys is illustrated in Fig. 40. The unit energy to propagate a crack in notched tear specimens, which is a measure of toughness, was determined for several stages of precipitation heat treatment, from the T4 or naturally aged temper to the T6 and for overaged tempers. For a spe-

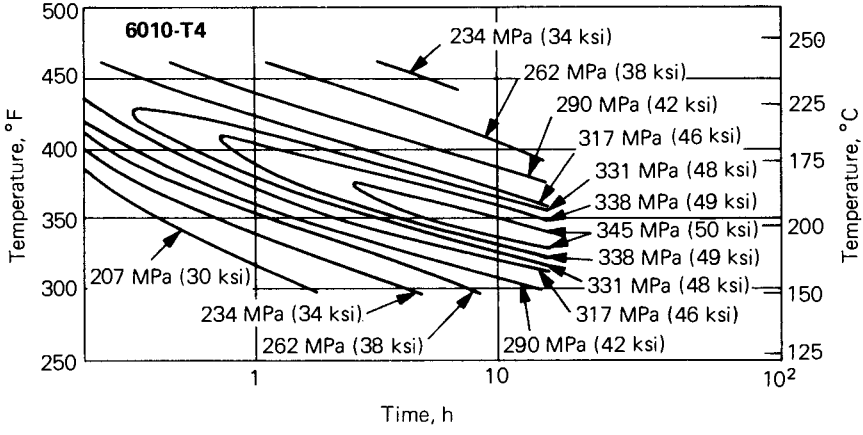

Fig. 38. Effect of aging time and temperature on longitudinal yield strength of 6010-T4.

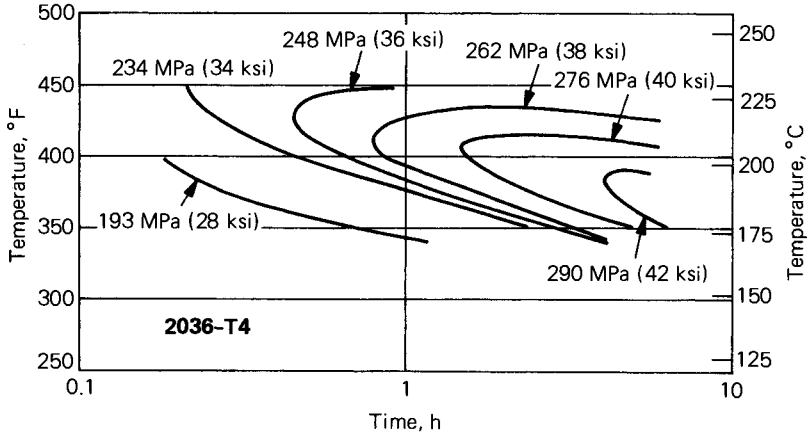

Fig. 39. Effect of aging time and temperature on longitudinal yield strength of 2036-T4.

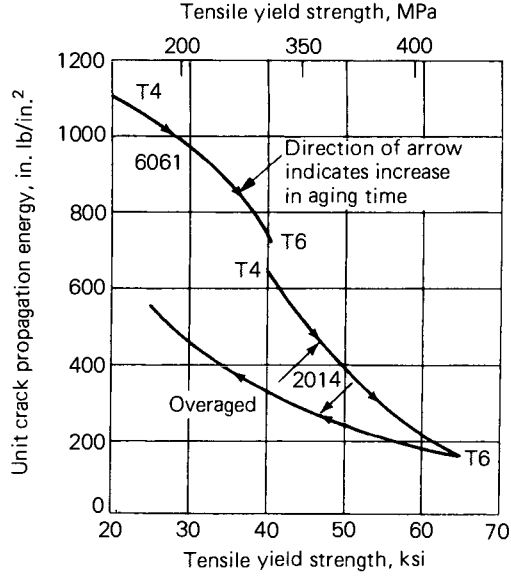

Fig. 40. Effects of precipitation heat treatment on unit crack propagation energy and yield strength of 2014 and 6061 alloys. (J.A. Nock, Jr. and H.Y Hunsicker, Journal of Metals, *Vol 15, 1963, p 216-224)*

cific yield strength, 2014 exhibited higher toughness in the underaged conditions than in the overaged condition. Different investigators found different effects of aging on the toughness of alloy 7075. In one investigation, the toughness of overaged 7075 was found to be lower than when it was underaged to the same yield strength (Ref 31). In another investigation of several lots of 7075, the toughness of material in underaged and overaged tempers was virtually identical, and toughness of a

high-purity variant of 7075 was superior in the overaged condition (Ref 32). In the instances where toughness was different at the same yield strength, the materials having the lower toughness exhibited a higher proportion of intergranular fracture. The reasons for the different results are tentatively attributed to differences in heating rate to the overaging temperature affecting the width of the precipitate-free zone at grain boundaries. Effects of cold work after solution heat treatment are opposite in 2XXX and 7XXX alloys (Ref 32). Cold work improves the combination of strength and toughness in 2024 (Fig. 41) and decreases it in overaged tempers of 7050 (Fig. 42). The improvement in 2024 is attributed to the refinement of the S' precipitate. This refinement in microstructure provided a simultaneous increase in strength and toughness. The negative effect of cold work in 7050 is attributed to the nucleation of coarse η' precipitates on dislocations, thereby decreasing strength without correspondingly improving toughness.

Because all heat treatable alloys overage with extended heating, the decrease in strength with time must be considered in selecting alloys and tempers for parts subjected to elevated-temperature service. Heat treatable alloys used as electrical conductors, such as 6101 or 6201, are frequently used in overaged tempers because of the higher electrical conductivity associated with more advanced decomposition of the solid solution.

Corrosion Resistance. The extent of precipitation during elevated-temperature aging of alloys 2014, 2219, and 2024 markedly influences

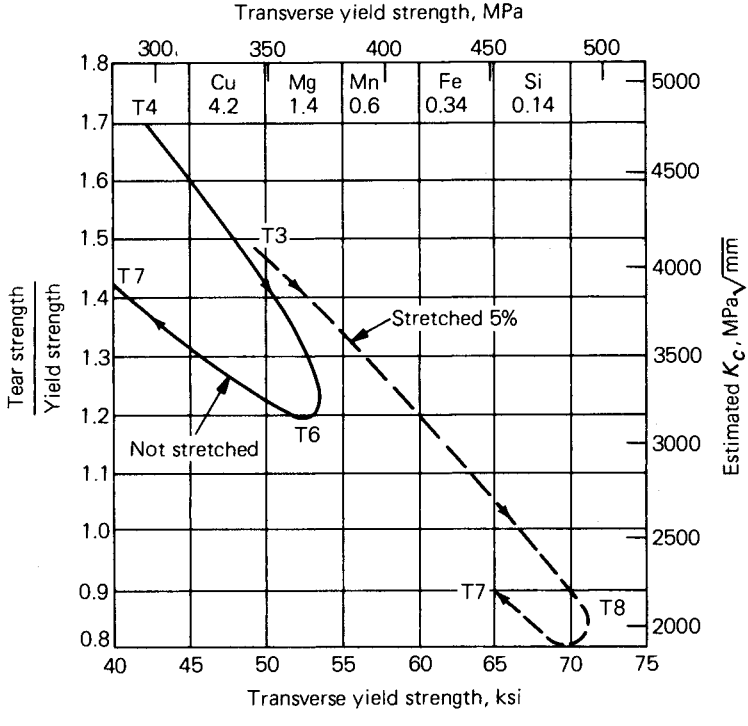

Fig. 41. Effect of stretching and aging on the toughness of 2024 sheet.

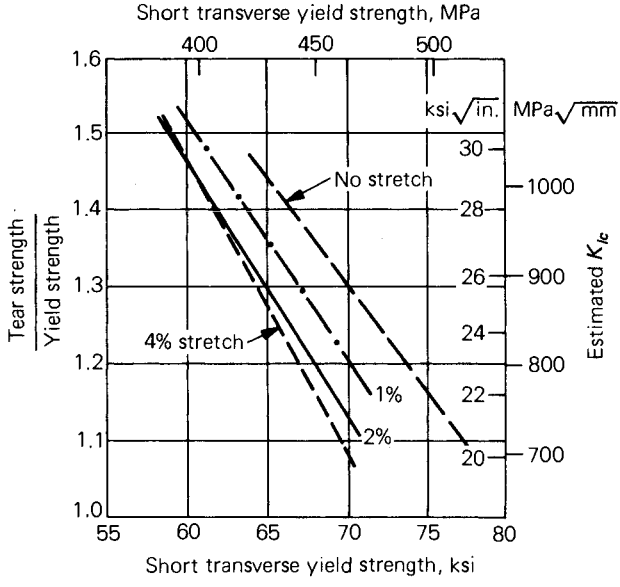

Fig. 42. Effects of stretching on the relationship between strength and notch toughness of alloy 7050 plate.

the type of corrosion attack and the corrosion resistance. With thin-section products quenched at rates sufficiently rapid to prevent precipitation in the grain boundaries during the quench, short periods of precipitation heat treating produce localized grain boundary precipitates adjacent to the depleted areas, producing susceptibility to intergranular corrosion. Additional heating, however, induces extensive general precipitation within the grains, lowering the corrosion potential differences between the grains and the boundary areas, thus removing the cause of the selective corrosion. To illustrate, changes in corrosion potential and corrosion resistance of 2024-T3 sheet with time and temperature of aging are charted in Fig. 43.

Fortunately, the extent of precipitation required to restore good corrosion resistance essentially coincides with that needed to develop maximum strength in some alloys. For products of thicker section, such as plate, extrusions, and forgings that cannot be quenched with sufficient rapidity to achieve the most favorable structures, commercial precipitation treatments also improve corrosion resistance.

Effect of Precipitation on Directional Properties of Extrusions. Extruded products that remain unrecrystallized after solution heat treating exhibit greater directional differences in mechanical properties than are shown by most other wrought products. These extrusions have a highly developed preferred orientation, with ⟨111⟩ and ⟨001⟩ axes parallel to the direction of extrusion. The directional variation in tensile properties correlates with the relative degree of alignment between planes of maximum shear stress and crystallographic slip planes (Ref 33). In extrusions of alloy 2024 that are straightened by stretching, the variation in preferred

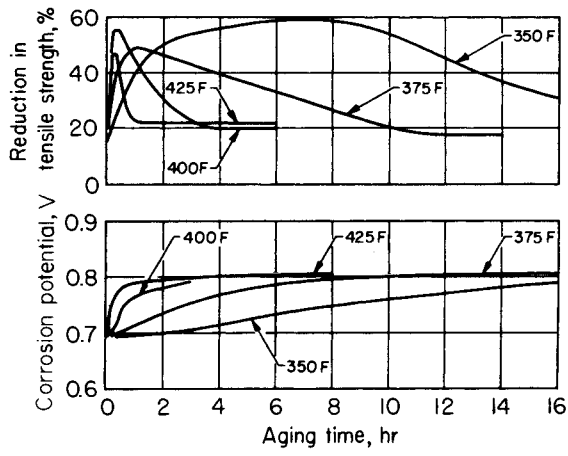

Fig. 43. Effect of precipitation heat treating on corrosion potential and corrosion resistance of alloy 2024-T3 sheet. Corrosion potential is measured in 53 g/L (7 oz/gal) NaCl and 9 mL/L (1.2 fluid oz/gal) of 30% H_2O_2 against a 0.1N calomel electrode.

orientation effect with section thickness tends to outweigh the influence of thickness on quenching rate, so that in naturally aged tempers the strength increases with increasing section thickness to about 3.75 cm (1.5 in.). When precipitation heat treatments are applied, the changes in tensile properties in the longitudinal and transverse directions are different, as indicated in Fig. 44. The anisotropy is reduced during precipitation by a decrease in high longitudinal tensile strength, coincidental with an improvement in tensile strength in the transverse direction. Precipitation heat treated tempers are used for extrusions of these alloys when higher transverse strengths and better corrosion resistance are advantageous.

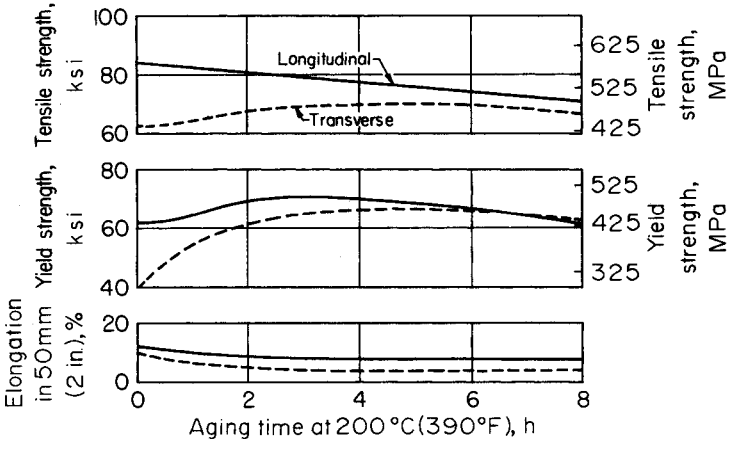

Fig. 44. Effect of precipitation heat treating at 200 °C (390 °F) on directional tensile properties of 32-mm (1 1/4-in.) thick 2024-T3 extruded shape.

ARTIFICIAL AGING OF 7XXX ALLOYS

Peak Strength. As illustrated by Fig. 35, aluminum-zinc-magnesium and aluminum-zinc-magnesium-copper alloys do not exhibit a stable W temper. Strengths increase over a period of many years by the growth of GP zones. Stable properties, higher strengths, improved corrosion resistance, and a lower rate of growth of fatigue cracks are obtained by the use of elevated-temperature aging. In contrast to the 2XXX and 6XXX series, which are aged at 170 to 190 °C (340 to 375 °F), temperatures of 115 to 130 °C (240 to 260 °F) are usually used for obtaining T6 properties with the 7XXX alloys. The reason is that in most cases, they provide high strength in reasonably short aging cycles. Aging curves are shown in Fig. 45 for rapidly quenched sheet of alloy 7075 that was brought slowly to the aging temperatures of 120 to 150 °C (250 to 300 °F). Under these conditions, peak strength was developed at 120 °C (250 °F).

Because of the nature of hardening precipitates, many variables are important to consider when aging 7XXX alloys. One variable that must be recognized is the time interval at room temperature between quenching and the start of the precipitation treatment. As shown in Fig. 46, the influence of this variable is specific for a given alloy composition. For 7178, the highest strengths are obtained with a minimum delay between quenching and aging. This is also true of 7075, but delays of 4 to 30 h are more detrimental than longer delays. The reasons for these effects are not completely understood, but there is an apparent relation to the degree of supersaturation existing in the quenched state and to reversion of GP zones during artificial aging (Ref 6 and 7). The effects of a natural aging interval for 7075-T6 sheet are eliminated by use of the two-step treatments, such as 4 h at 100 °C (212 °F) plus 8 h at 160 °C (315 °F). This treatment develops the same strength in 7075 sheet as that provided by 24 h at 120 °C (250 °F), despite the fact that isothermal aging above 250 °F usually provides much lower strength. The reason is that the treatment at 100 °C (212 °F) develops a distribution of GP zones that is stable when

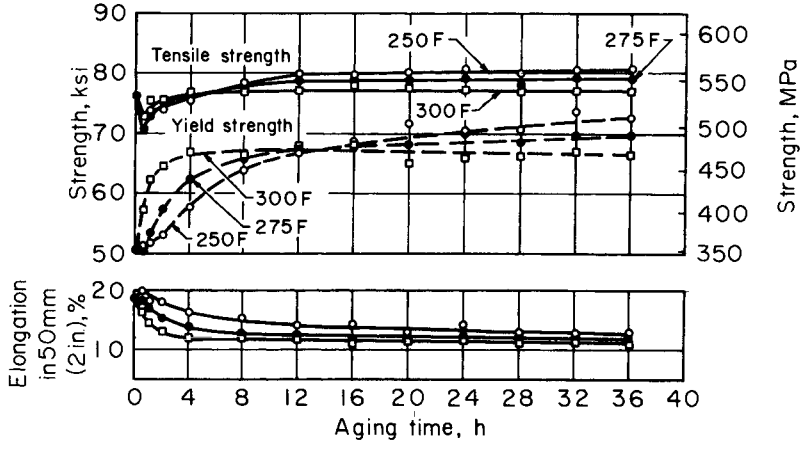

Fig. 45. Aging of 7075 sheet at 120 to 150 °C (250 to 300 °F). (J.A. Nock, Jr., Alcoa Research Laboratories)

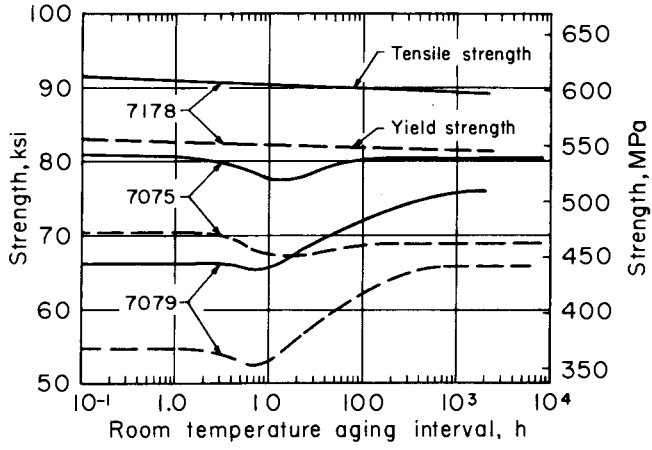

Fig. 46. Effect of time interval at room temperature between quenching and precipitation heat treating on tensile and yield strengths of 7178-T6, 7075-T6, and 7079-T6 alloy sheet. (J.A. Nock, Jr., Alcoa Research Laboratories)

the temperature is raised (Ref 34). When the quench rate is lowered, as in quenching thick forgings in hot water, homogeneous nucleation becomes difficult even at temperatures as low as 120 °C (250 °F), or even lower. Under these conditions, a preage near 100 °C (212 °F) before the age near 120 °C (250 °F) increases strength (Ref 35). Another variable to be considered, then, is quench rate and first-step aging conditions. The copper-free 7XXX alloys such as 7005 also use two-step aging practices to provide high strength. A standard treatment for 7005 extrusions is 8 h at 110 °C (225 °F), followed by 16 h at 150 °C (300 °F). Slow heating to the aging temperature acts like a first step in that it permits GP zones to grow to a size that does not dissolve at higher temperatures. Consequently, heating rate is an important factor. One standard treatment for 7039 calls for a controlled rate of heating.

Overaged Tempers. During the early 1960's, T7X-type practices were developed to improve the corrosion resistance of the 7XXX alloys containing more than 1% copper. The T73 temper was developed to improve the short-transverse stress-corrosion cracking resistance of 7075 thick section products (Ref 22). The T76 temper was applied to 7075 and 7178 for improved resistance to exfoliation corrosion (see Chapter 7 of this Volume). Since that time, T7 tempers have been developed for later generation 7XXX alloys such as 7475, 7049, and 7050. These tempers are based on the fact that selective corrosion at grain boundaries is reduced with increased overaging. Aging temperatures in the range 160 to 175 °C (325 to 350 °F) are used following a controlled exposure at lower temperatures to allow the formation of large numbers of GP zones that are stable at the higher temperatures. The zones transform to the intermediate η' precipitate and finally to the equilibrium η ($MgZn_2$) phase during overaging. Eliminating the first step and rapidly heating to the final aging temperature results in low strength, because of reversion of the GP zones and insufficient nuclei for the formation of a fine dispersion of η. As

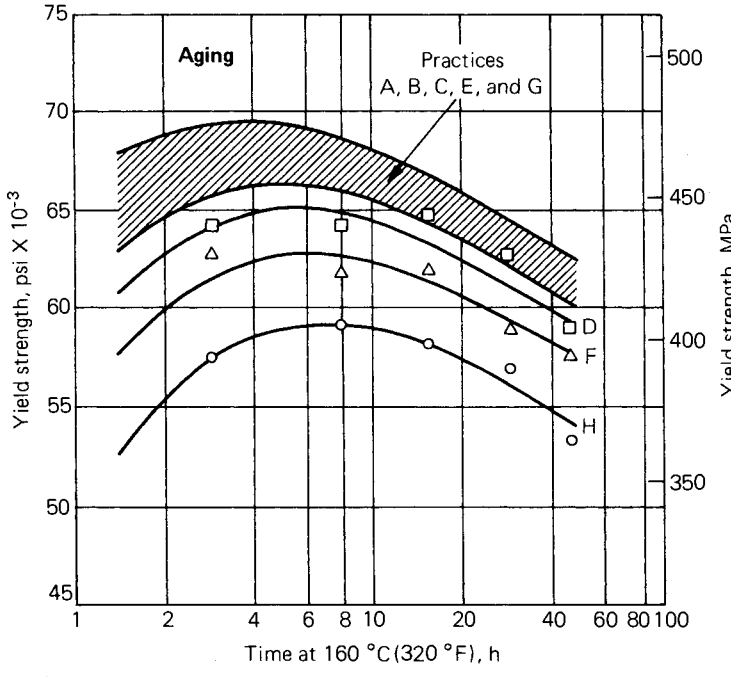

Two-step aging	Single-step aging	Heating method	Heating rate °C/min	Heating rate °F/min
A	B	Programmed air oven	0.23 ± 0.01	0.4 ± 0.02
C	D	Programmed air oven	0.93 ± 0.03	1.7 ± 0
E	F	Air oven at 160 °C (320 °F)	~10	~18
G	H	Oil bath at 160 °C (320 °F)	~100	~180

Fig. 47. The influence of processing variables on 7075 aging curves.

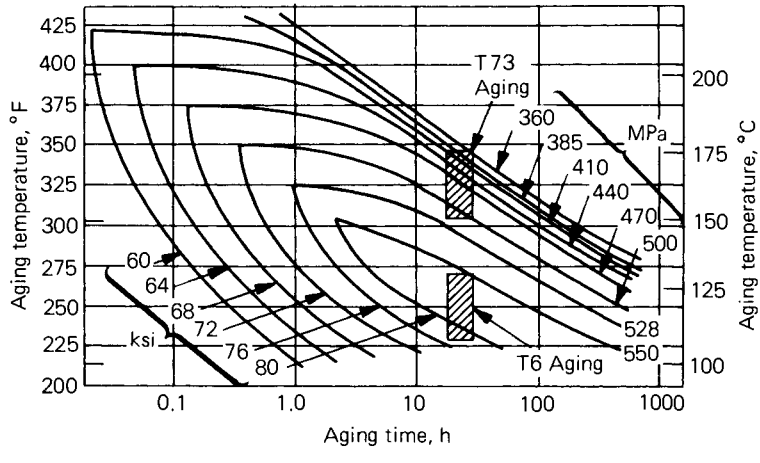

Fig. 48. ISO yield strength curves for 7075.

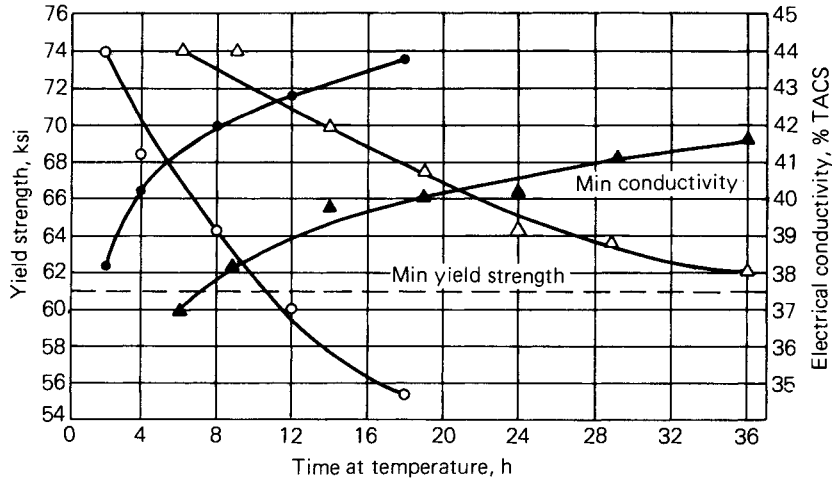

Fig. 49. Second-step aging curves for 100-mm (4-in.) 7050 plate.

shown in Fig. 47, the use of either a slow heating rate or a two-step aging practice overcomes this problem (Ref 36). Greatly extending the natural aging interval also permits GP zones to grow to a size that resists reversion, even with rapid heating, but this extended time at room temperature is not practical (Ref 34). Consequently, suggested commercial practices normally involve heating to the temperature range of 100 to 120 °C (210 to 250 °F) and soaking 1 to 24 h before exposure at the higher temperature. Numerous combinations of time and temperature are possible during the second-step age, as shown in Fig. 48. In any case, overaging can occur rather rapidly, as shown in Fig. 49. Therefore, extraordinary process control is required.

To assist with the control problem, a new method has been developed that gives a quantitative description of effects of precipitation during overaging (Ref 37). The method is based on the observation that the overaging reaction is isokinetic (Fig. 50) (Ref 38). These effects can be described by the following equation:

$$S = Y \exp - \left(\frac{t_s}{F} + \phi\right) \qquad \text{Eq 10}$$

where S is yield strength; Y is a term having units of strength and that is alloy, fabrication practice, and test direction dependent; t_s is the time at soak temperature; F is a temperature-dependent term; and

$$\phi = \int \frac{dt}{F} \qquad \text{Eq 11}$$

where t is time during heating. These relationships provide the furnace operator with a method of compensating for heating rate and for differ-

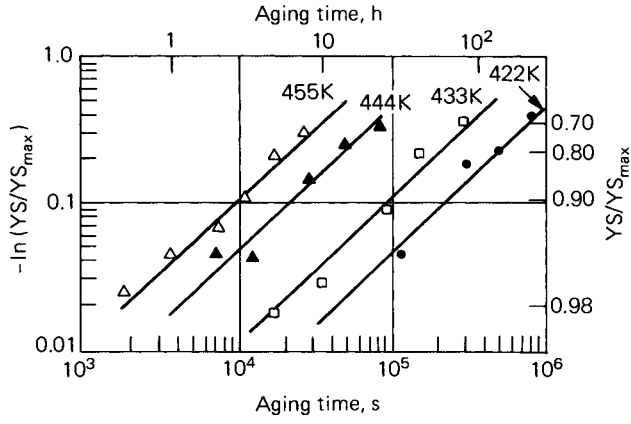

Fig. 50. Overaging kinetics of alloy 7050.

ences in soak temperature between that desired and that attained. The information provided by solving these equations can be used in a variety of ways. One way is to transfer the solutions to a series of graphs and read the answers off the graphs. Other ways are to program and use a pocket calculator or to use a patented process (Ref 39).

High temperature aging practices also are used with the lower copper or copper-free 7XXX alloys such as 7004, 7005, 7021, and 7039. In general, these practices are used to obtain the best combination of strength, corrosion resistance, and toughness. While stress-corrosion performance in the longitudinal and long-transverse directions is relatively high, resistance to stress-corrosion cracking in the short-transverse direction is less than that obtained by aging the 7XXX alloys containing higher copper by T7X-type practices.

Thermomechanical aging (TMA) involves deformation after solution heat treatment. The deformation step may be warm or cold and before, after, or during aging. The simplest TMA practices are those of the conventional T3, T8, or T9 tempers. The rate and extent of strengthening during precipitation heat treatment are distinctly increased in some alloys by cold working after quenching, whereas other alloys show little or no added strengthening when treated by this sequence of operations (Ref 40). Alloys of the 2XXX series such as 2024, 2124, and 2219 are particularly responsive to cold work between quenching and aging, and this characteristic is the basis for the higher strength T8 tempers. The strength improvement accruing from the combination of cold working and precipitation heat treating is a result of nucleation of additional precipitate particles by the increased strain. The effect on the precipitate shape of artificially aging 2024 from three initial conditions is given in Fig. 51: that of aging of 2024-T4, which is not cold worked; that of 2024-T3, cold worked equivalent to a 1 to 2% reduction; and that of 2024-T361, cold worked 5 to 6%. The *S'* precipitate platelets in Fig. 51(a), which shows the structure of 2024-T6 having a nominal yield strength of 400 MPa (58 ksi), were nucleated exclusively by dislocation loops resulting from condensation of vacancies about dispersoid particles during quenching. The much

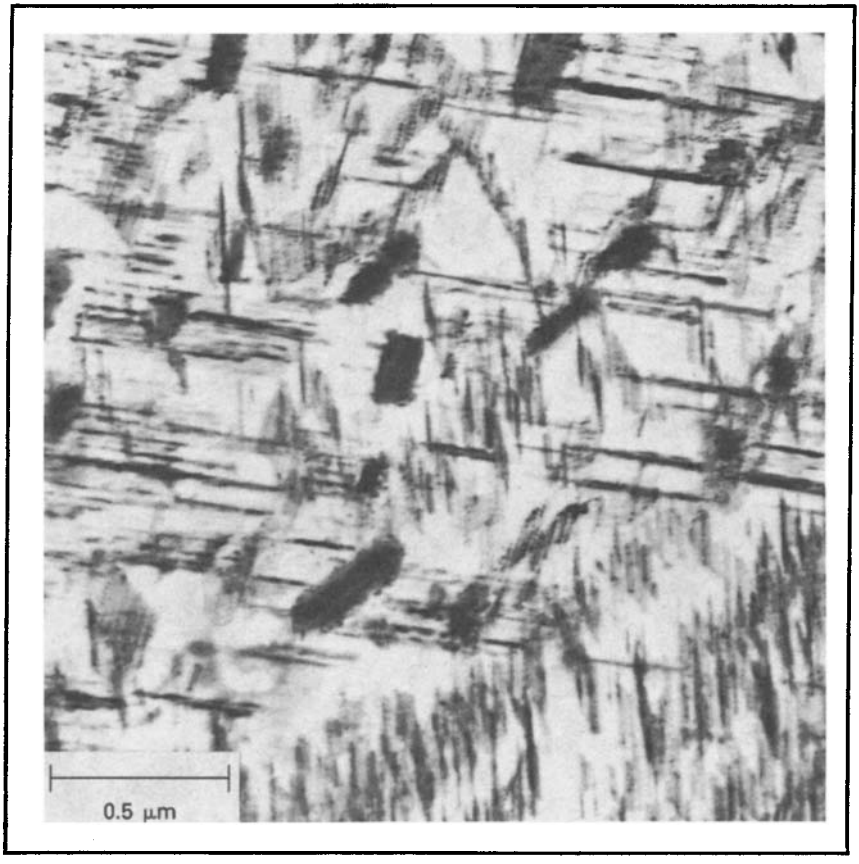

Fig. 51a. Electron transmission micrograph of 2024-T6, solution heat treated, quenched, aged 12 h at 190 °C (375 °F). (50,000×).

finer, more numerous, precipitate particles apparent in Fig. 51(b), representing 2024-T81 with a yield strength of 455 MPa (66 ksi), and Fig. 51(c), the structure of 2024-T861 having a yield strength of 500 MPa (73 ksi), were nucleated by the extensive network of additional dislocations introduced by cold working after quenching.

Normally, cold work is introduced by stretching; however, other methods such as cold rolling can be used. Recently, 2324-T39 was developed. The T39 temper is obtained by cold rolling approximately 10% after quenching followed by stretching to stress relieve. This type of approach results in strengths similar to those obtained with T8 processing but with the better toughness and fatigue characteristics of T3 products.

Various combinations of cold working or warm working after quenching, followed by natural or artificial aging, have been tried with 2XXX alloys (Ref 41). Regardless of the working practice, artificial aging progressively decreases toughness and fatigue performance but improves the corrosion resistance of 2XXX alloys. Therefore, the choice of practice depends on application design conditions.

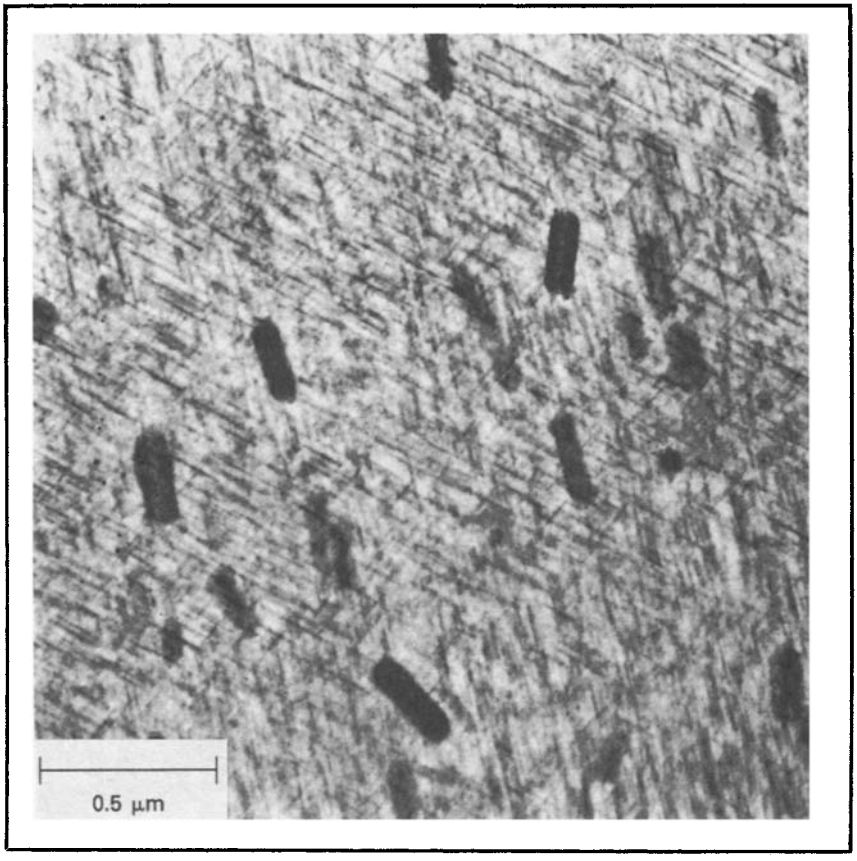

Fig. 51b. Electron transmission micrograph of 2024-T81, solution heat treated, quenched, stretched 1.5%, aged 12 h at 190 °C (375 °F). Precipitate platelets are smaller and more numerous than in (a). (50,000×).

Cold work after solution heat treatment affects the aging response of 7XXX alloys. Because amounts of cold work are usually introduced for mechanical stress relieval, the effect on properties obtained by aging for a T6 treatment of 24 h at 120 °C (250 °F) is minimal (Fig. 52). The same amount of cold work, however, significantly reduces the strength obtainable by T7-type aging. The data in Fig. 52 reveal that the effect is not because of a change in the rate of overaging. Rather, cold work decreases the maximum attainable strength. The attainable strength decreases progressively with increasing cold work up to at least 5%. This effect is attributed to the effect of dislocations on heterogeneously nucleating η' precipitate. Cold working by cold rolling to levels higher than those used for stress relief purposes can provide hardness levels surpassing those provided by precipitation hardening effects (Fig. 53), but these treatments are not used commercially.

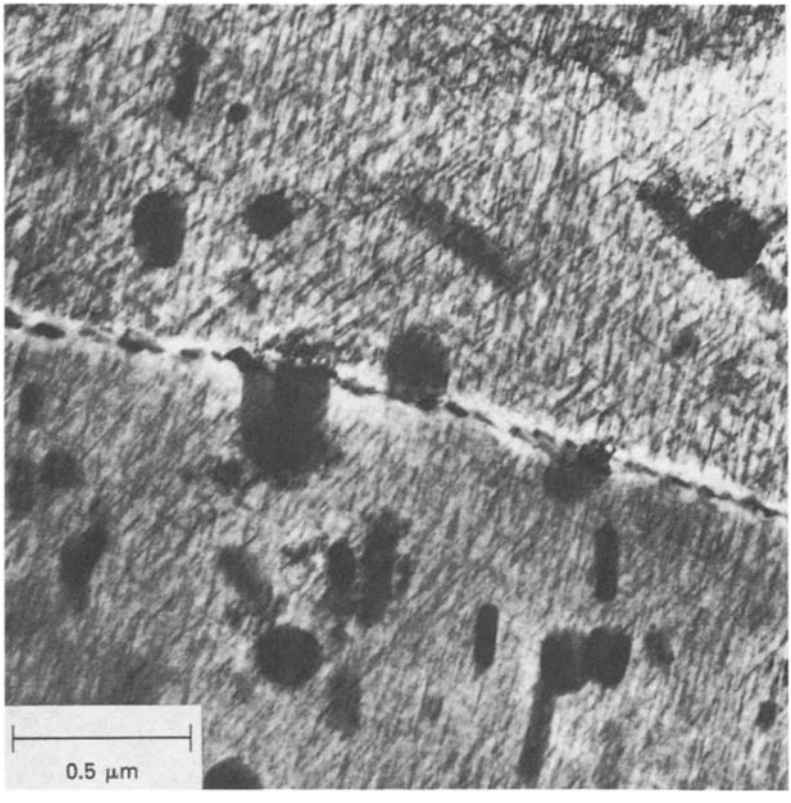

Fig. 51c. Electron transmission micrograph of 2024-T86, solution heat treated, quenched, cold rolled 6%, aged 12 h at 190 °C (375 °F). Precipitate platelets are smaller and more numerous than in (b). (50,000×).

Considerable experimentation has been conducted on the effects of final thermomechanical treatments (FTMT) on the performance of 7XXX alloys, in an attempt to provide more attractive combinations of strength, toughness, and resistances to fatigue and stress-corrosion cracking (Ref 42-44). This type of processing involves a preage after quenching and cold or warm working followed by a final age. No consensus exists as to the value of such processing at this time, nor has the use of FTMT been accepted commercially.

Precipitation Heat Treating Without Prior Solution Heat Treatment. Certain alloys that are relatively insensitive to cooling rate during quenching can be either air cooled or water quenched directly from a final hot working operation. In either condition, these alloys respond strongly to precipitation heat treatment. This practice is widely used in producing thin extruded shapes of alloys 6061, 6063, 6463, and 7005. Upon precipitation heat treating after quenching at the extrusion press, these alloys

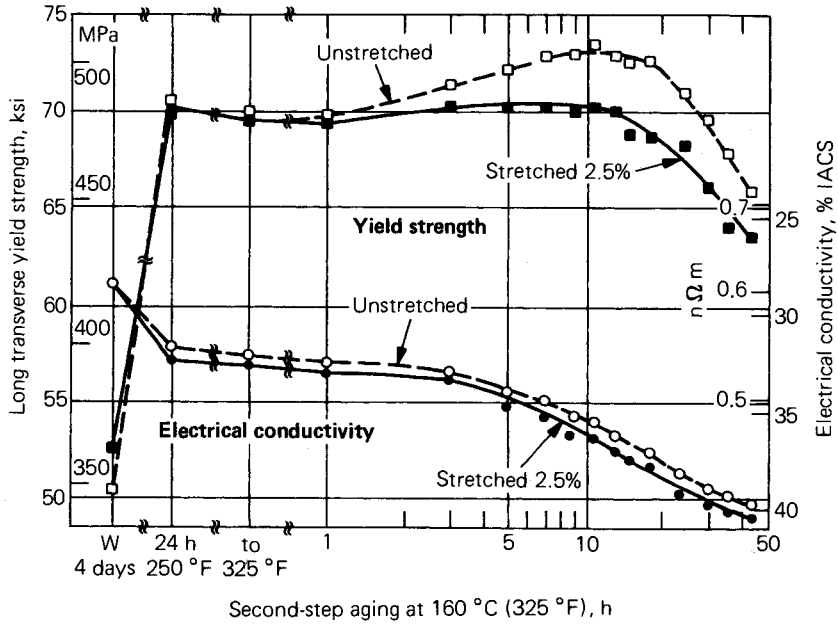

Fig. 52. Effect of stretching on aging response of 10-mm ($^3/_8$-in.) thick 7475 plate.

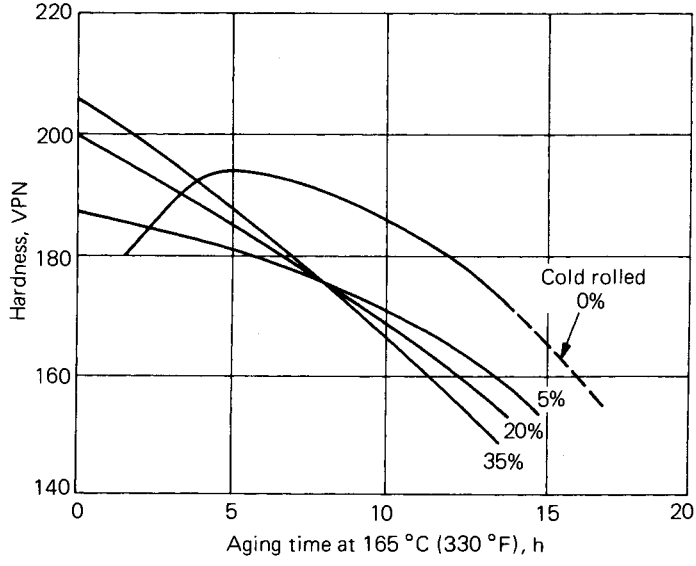

Fig. 53. The effect of cold work on the aging kinetics of a 7075-type alloy.

develop strengths nearly equal to those obtained by adding a separate solution heat treating operation. Changes in properties occurring during the precipitation treatment follow the principles outlined in the discussion of solution heat treated alloys.

Precipitation Heat Treating Cast Products. The mechanical properties of permanent mold, sand, and plaster castings of most alloys are greatly improved by solution heat treating, quenching, and precipitation heat treating, using practices analogous to those used for wrought products. In addition to this sequence of operations, used to establish tempers of the T6 and T7 types, precipitation heat treatment can be used without prior solution heat treating to produce T5-type tempers. The effects of precipitation treatment on mechanical properties have the same characteristic features cited for wrought products. The use of either T5 or T7 overaging treatments is more prevalent for cast than for wrought products. These treatments, which result in lower strength and hardness than are obtained in the T6 temper, are used to minimize dimensional changes during elevated-temperature service. Thermal treatments are not generally beneficial to the mechanical properties of die castings, and therefore usually are not applied to them.

Representative effects of precipitation heat treating on the tensile properties of the widely used aluminum-silicon-magnesium alloy 356 are illustrated in Fig. 54. Higher strengths and superior ductility are obtained by solution heat treating before precipitation heat treating than by precipitation heat treating directly from the as-cast condition (F temper). Because of the finer cast structure of the more rapidly solidified permanent mold castings, their tensile properties are superior to those of sand castings similarly heat treated.

Effect of Precipitation Heat Treating on Residual Stress. The stresses developed during quenching from solution heat treatment are reduced during subsequent precipitation heat treatment. The degree of relaxation of stresses is highly dependent upon the time and temperature of the precipitation treatment and the alloy composition. In general, the precipi-

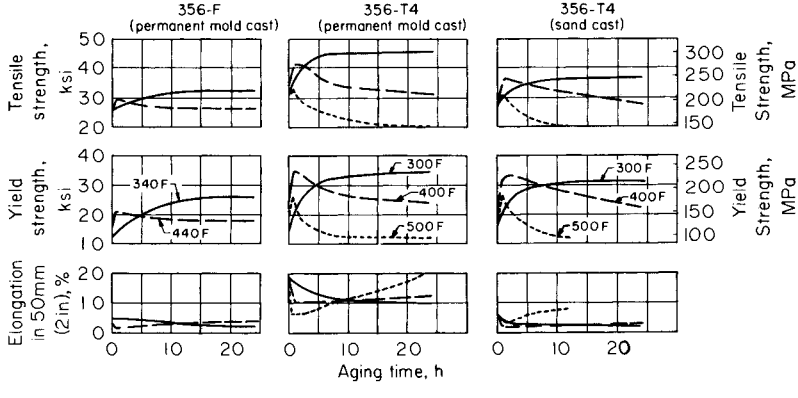

Fig. 54. Elevated-temperature aging characteristics of cast 356. Temper designations given apply before aging.

tation treatments used to obtain the T6 tempers provide only modest reduction in stresses, ranging from about 10 to 35%. To achieve a substantial lowering of quenching stresses by thermal stress relaxation, higher temperature treatments of the T7 type are required. These treatments are used when the lower strengths resulting from overaging are acceptable. Specific methods for reducing the residual stresses in heat treated products by both mechanical and thermal treatment are described in Volume III in Chapter 10 of *Aluminum* published by ASM in 1967.

The relaxation of stress under constant strain is essentially the conversion of elastic to plastic strain, by the same mechanisms involved in creep. The deformation accomplished by this means is used to establish precise final dimensions in large welded tanks. Primary forming of alloy 2219 tank segments is accomplished in the solution heat treated and cold worked T37 temper, followed by assembly welding. The achievement of final contours and dimensions of the welded assembly is facilitated by performing the precipitation heat treatment of 24 h at 165 °C (325 °F) to the T87 temper while the assembly is clamped in a contour-restraining fixture. In the restrained condition, the alloy yields, assuming the shape imposed by the fixture.

DIMENSIONAL CHANGES IN HEAT TREATING

In addition to the completely reversible changes in dimensions that are a simple function of temperature change and the thermal expansion coefficients, expansions and contractions of a more permanent character are encountered during heat treatment (Ref 45). These changes are of a metallurgical nature, arising from the introduction and relaxation of stresses, recrystallization, and solution or precipitation of alloying elements. Elements that decrease the lattice spacing when in solid solution generally cause a decrease in dimensions, because solution is affected during solution heat treating. During subsequent precipitation at elevated temperatures, a reversal of this change is expected. Because certain elements expand the lattice and others contract it, these effects vary considerably with the proportions of different elements used in commercial alloys. These solution and precipitation effects are primarily nondirectional in nature.

Other important effects that may be highly directional are those associated with relief of residual stresses introduced during fabrication, or with development of residual stresses during quenching. The degree of directionality is dependent to a major extent upon the type, shape, and section thickness of the product, the nature of the quenching medium, and the manner in which quenching is performed. The dimensional changes associated with recrystallization vary with the type and extent of prior working, and the degree of anisotropy varies with preferred orientation. These factors are subject to so much variation that there is no valid generalization regarding specific changes that may be expected in different products.

Results obtained in laboratory experiments are summarized in Fig. 55. A sequence of thermal treatments was applied to sheet and extruded rod of four alloys, and the unit dimensional changes were determined after each step. These data demonstrate certain characteristic differences among compositions. In addition, directional effects result from stresses present

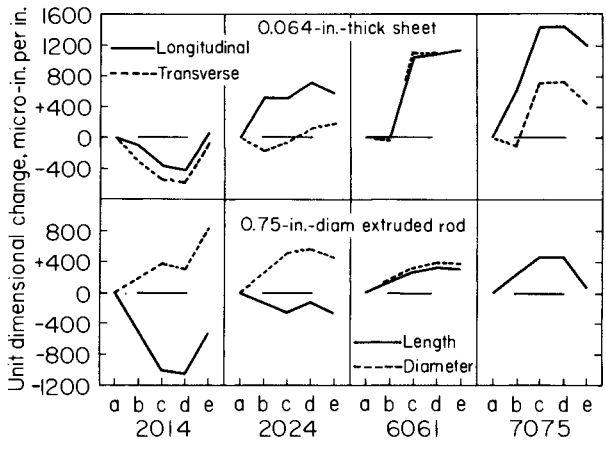

Fig. 55. Effects of heat treatments on dimensional changes in sheet and extruded rod. (a) As fabricated. (b) Annealed. (c) Solution heat treated and quenched in cold water. (d) Naturally aged, T4. (e) Precipitation heat treated, T6. (L.A. Willey, Alcoa Research Laboratories)

in the as-fabricated condition, as well as those introduced by quenching, which vary with the shape and type of product.

Dimensional changes occurring during room temperature aging of cold water quenched sheet are illustrated in Fig. 56 for four alloys. The direction of initial change is, in some cases, opposite to that consistent with a reduction in solute concentration of the solid solution. The existence of such changes and of the subsequent reversal was verified, however, by careful dilatometric measurements. The changes are small, but of sufficient magnitude so that tempers more stable dimensionally are sometimes preferred for parts used in instruments or apparatus requiring maximum dimensional stability.

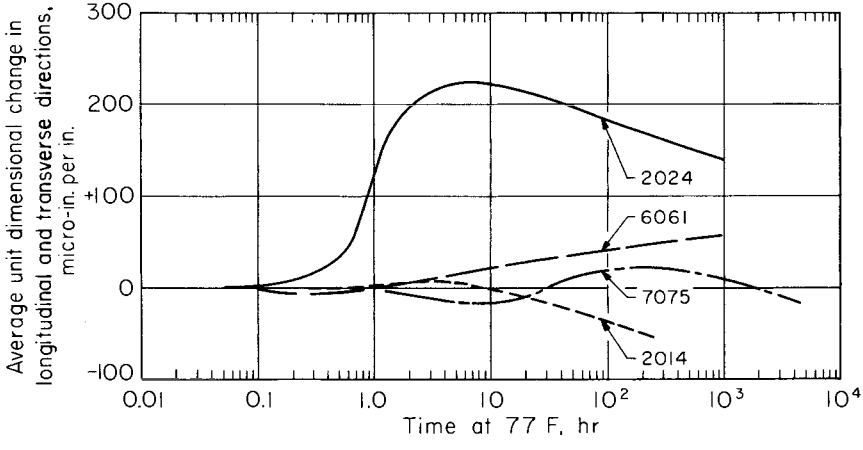

Fig. 56. Average unit dimensional changes during room temperature aging of cold water quenched sheet. (L.A. Willey, Alcoa Research Laboratories)

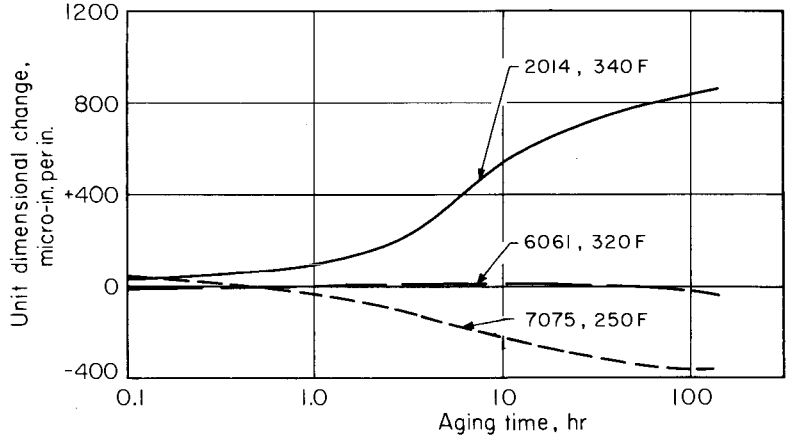

Fig. 57. Effects of unit dimensional changes of time at precipitation heat treating temperatures used to produce the T6 temper of three alloys. (L.A. Willey, Alcoa Research Laboratories)

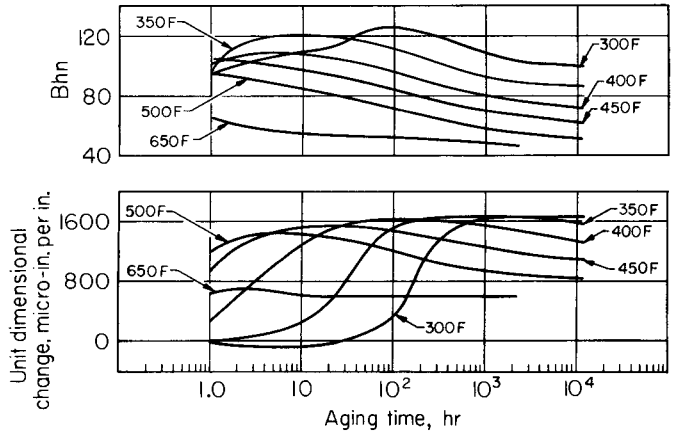

Fig. 58. Unit dimensional changes and hardness of aluminum-copper-manganese-silicon alloy 2025-T4, precipitation heat treated at six temperatures. (M.W. Daugherty, Alcoa Research Laboratories)

Unit dimensional changes that accompany precipitation heat treating three alloys at the temperature used for producing the T6 temper in each alloy are charted in Fig. 57. These effects are normally not directional, although evidence was found that some anisotropy may be encountered in products having a high degree of preferred orientation. Growth in dimensions as a result of precipitation is greatest for alloys containing substantial amounts of copper, but is reduced progressively with increasing magnesium content in such aluminum-copper-magnesium alloys as 2014 and 2024. The aluminum-magnesium-silicon alloy 6061 shows little dimensional change during precipitation heat treatment, whereas aluminum-

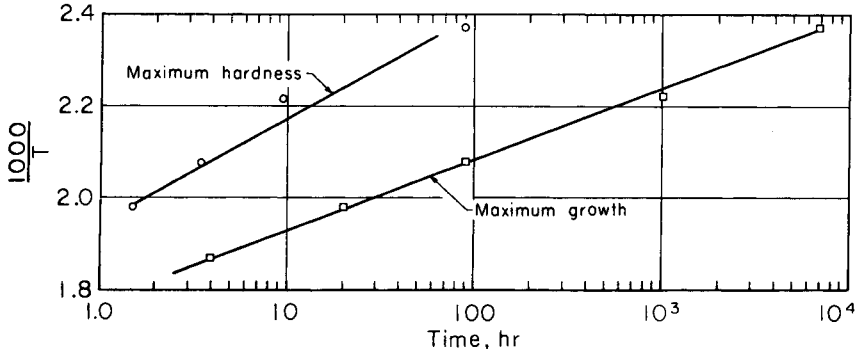

Fig. 59. Variation in time to produce maximum hardness and maximum growth during precipitation heat treating of 2025-T4, as a function of the reciprocal of absolute temperature.

zinc-magnesium-copper alloy 7075 actually contracts.

These effects assume considerable importance for parts that must maintain a precision fit over long periods of operation at elevated temperature, such as engine pistons. The thermal treatments used for such parts are designed to promote growth during the heat treating operation, avoiding this change during service. To accomplish this, the precipitation treatment must be at a temperature high enough so that the hardness and strength of the product are lower than if dimensional stability were not the critical objective.

The effects of time and temperature for precipitation heat treatment on the unit dimensional change and Brinell hardness of the aluminum-copper-manganese-silicon alloy 2025-T4 are demonstrated in Fig. 58. The extent of aging required to produce maximum hardness or strength at a specific temperature is much shorter than that needed to develop the maximum dimensional change. This is also illustrated by reciprocal temperature plots of the data (Fig. 59). The contraction that follows the attainment of maximum growth at temperatures of 175 °C (350 °F) or higher is attributed to transformation of the transition precipitate to the equilibrium structure. It also may be influenced by changes in coherency with growth and coalescence of the precipitate particles.

REFERENCES

1. "Vacancies and Other Point Defects in Metals and Alloys", Institute of Metals Monograph and Report Series No. 23, 1958
2. H. Jagodzinski and F. Laves, Uber Die Deutung der Entmischungsvorgange in Mischkristallen unter besonder Berucksichtigung der Systeme Aluminium-Kupfer und Aluminium-Silber, *Zeitschrift fur Metallkunde*, Vol 40, 1949, p 296-305
3. F. Seitz, in *L'Etat Solide*, Stoopes, Brussels, 1952, p 401
4. R.B. Nicholson, G. Thomas, and J. Nutting, Electron Microscopic Studies of Precipitation in Aluminum Alloys, *Journal of the Institute of Metals*, Vol 87, 1958-1959, p 429-488
5. J.D. Embury and R.B. Nicholson, The Nucleation of Precipitates: The System Al-Zn-Mg, *Acta Metallurgica*, Vol 13, 1965, p 403-417
6. D.W. Pashley and M.H. Jacobs, The Mechanism of Phase Transformation

in Crystalline Solids, London, Institute of Metals, Monograph 33, 1969
7. J.D. Embury and R.B. Nicholson, The Mechanism of Phase Transformation in Crystalline Solids, London, Institute of Metals, Monograph 33, 1969
8. A. Kelly and R.B. Nicholson, Precipitation Hardening in *Progress in Materials Science,* Vol 10, Edited by B. Chalmers, New York: Macmillan, 1963
9. E.A. Starke, Jr., The Causes and Effects of Denuded or Precipitate-Free Zones at Grain Boundaries in Aluminum-Base Alloys, *Journal of Metals,* Jan 1970
10. N. Ryum, Precipitation Kinetics in an Al-Zn-Mg Alloy, *Zeitschrift fur Metallkunde,* Vol 64, Feb 1975, p 338-343
11. G. Thomas and J. Nutting, Electron Microscopic Studies of Precipitation in Aluminum Alloys, in "The Mechanisms of Phase Transformations in Metals", Institute of Metals Monograph and Report Series No. 18, 1956, p 57-66
12. T.F. Bower, H.D. Brody, and M.C. Flemings, Effects of Solidification Variables on the Structure of Aluminum Base Ingots, Army Materials Research Agency Contract DA-19-020-ORD-5706A, Frankford Arsenal, Philadelphia, 1964
13. D. Altenpohl, Detailed Investigation on the Cast Microstructure of Aluminum and Aluminum Alloys, *Zeitschrift fur Metallkunde,* Vol 56, 1965, p 653-663
14. P.R. Sperry, The Relation Between Constitution and Ultimate Grain Size in Aluminum-1.25% Manganese Alloy 3003, *Transactions of ASM,* Vol 50, 1958, p 589-610
15. W.L. Fink and L.A. Willey, Quenching of 75S Aluminum Alloy, *Transactions of AIME,* Vol 175, 1948, p 414-427
16. J.W. Evancho and J.T. Staley, Kinetics of Precipitation in Aluminum Alloys During Continuous Cooling, *Metallurgical Transactions A,* Vol 5, Jan 1974, p 43-47
17. J.B. Austin, The Flow of Heat in Metals, American Society for Metals, 1942, p 91-138
18. J. Katz, A New Heat Treatment for Precipitation Hardening Aluminum Alloys, *Metal Progress,* Feb 1966, p 70-72
19. S.E. Axter, Effects of Interrupted Quenches on the Properties of Aluminum, Tech Paper CM80-409 Society of Manufacturing Engineers, 1980
20. L. Swartzendruber *et al,* Nondestructive Evaluation of Nonuniformities in 2219 Aluminum Alloy Plate—Relationship to Processing, National Bureau of Standards Report NBSIR 80-2069, Dec 1980
21. R.E. Sanders, Jr. and J.T. Staley, Relationships Between Microstructure, Conductivity, and Mechanical Properties of Alloy 2024-T4, *Aluminium,* Parts I and II, Dec 1982/Jan 1983/Feb 1983
22. United States Patent 3198676, Aug 1965
23. L.W. Kempf, H.L. Hopkins, and E.V. Ivanso, Internal Stress in Quenched Aluminum and Some Aluminum Alloys, *Transactions of AIME,* Vol 3, 1934, p 150-180
24. G. Forrest, Internal or Residual Stresses in Wrought Aluminum Alloys and Their Structural Significance, *Journal of the Royal Aeronautical Society,* Vol 58, April 1954, p 261-276
25. K.R. Van Horn, Residual Stresses Introduced During Metal Fabrication, *Journal of Metals,* March 1953, p 405-422
26. R.T. Torgerson and C.J. Kropp, Improved Heat Treat Processing of 7050 Aluminum Alloy Forgings Using Synthetic Quenchants, General Dynamics Convair Division Report, 1977
27. E.A. Lauchner, Glycol Quenching 7075 Forgings 2.5 Inches Thick, Aerospace Heat Treatment Committee Report R-3, Dec 1973
28. J.F. Collins and C.E. Maduell, Polyalkylene Glycol Quenching of Aluminum Alloys, Paper No. 28, Corrosion/77, March 1977, p 14-18
29. P. Archambault *et al,* Optimum Quenching Conditions for Aluminum Alloy Castings, Heat Treatment 1976—Proceedings of 16th International Heat Treatment Conference, Metals Society (London) Book 181, 1976, p 105-109, 219-220

30. United States Patent 3996075, Dec 1976
31. I. Kirman, *Metallurgical Transactions A*, Vol 2, 1971, p 1761-1770
32. J.T. Staley, Microstructure and Toughness of High-Strength Aluminum Alloys, "Properties Related to Fracture Toughness", ASTM STP 605, American Society for Testing and Materials, 1976, p 71-103
33. K.R. Van Horn, Factors Affecting Directional Properties in Aluminum Wrought Products, *Transactions of ASM*, Vol 35, 1944, p 130-155
34. J.T. Staley, R.H. Brown, and R. Schmidt, Heat Treating Characteristics of Al-Zn-Mg-Cu Alloys With and Without Silver, *Metallurgical Transactions A*, Vol 3, Jan 1972, p 191-199
35. S. DesPortes, E. Sanko, and K. Wolfe, "Effect of Quench Rate on Precipitate Nucleation in Aluminum Alloy 7075", Purdue University School of Materials Engineering, May 1980
36. R.F. Ashton and D.S. Thompson, Effect of Heating Rate on the Aging Behavior of 7075 Alloy, *Metallurgical Transactions A*, Vol 245, 1969, p 2101
37. J.T. Staley, Kinetics for Predicting Effects of Heat Treating Precipitation-Hardenable Aluminum Alloys, *Industrial Heating XLIV*, Oct 1977, p 6-9
38. J.T. Staley, Aging Kinetics of Aluminum Alloy 7050, *Metallurgical Transactions 5*, April 1974, p 929-932
39. United States Patent 3645804, 1972
40. E.H. Dix, Jr., New Developments in High Strength Aluminum Wrought Products, *Transactions of ASM*, Vol 35, 1944, p 130-155
41. D.S. Thompson, S.A. Levy, and G.E. Spangler, Thermomechanical Aging of Aluminum Alloys I and II, *Aluminium*, Jan 1974, p 647-649, 719-723
42. R.R. Sawtell, Effects of FTMT Versus Alloying on Fatigue and Fracture of 7XXX Alloy Sheet, Thermomechanical Processing of Aluminum Alloys, AIME Conference Proceedings, 1979
43. A.W. Sommer, N.E. Paton, and D.G. Folgner, Effects of Thermomechanical Treatments on Aluminum Alloys, Technical Report AFML-TR-72-5, Feb 1972
44. E. DiRusso *et al*, Thermomechanical Treatments on High Strength Al-Zn-Mg(Cu) Alloys, *Metallurgical Transactions 4*, April 1973, p 1133-1144
45. H.Y. Hunsicker, Dimensional Changes in Heat Treating Aluminum Alloys, *Metallurgical Transactions A*, May 1980, p 759-773